Quantification of postural stability in the healthy population as reference for future research on Dorsal Root Ganglion stimulation in Spinal Cord Injury patients

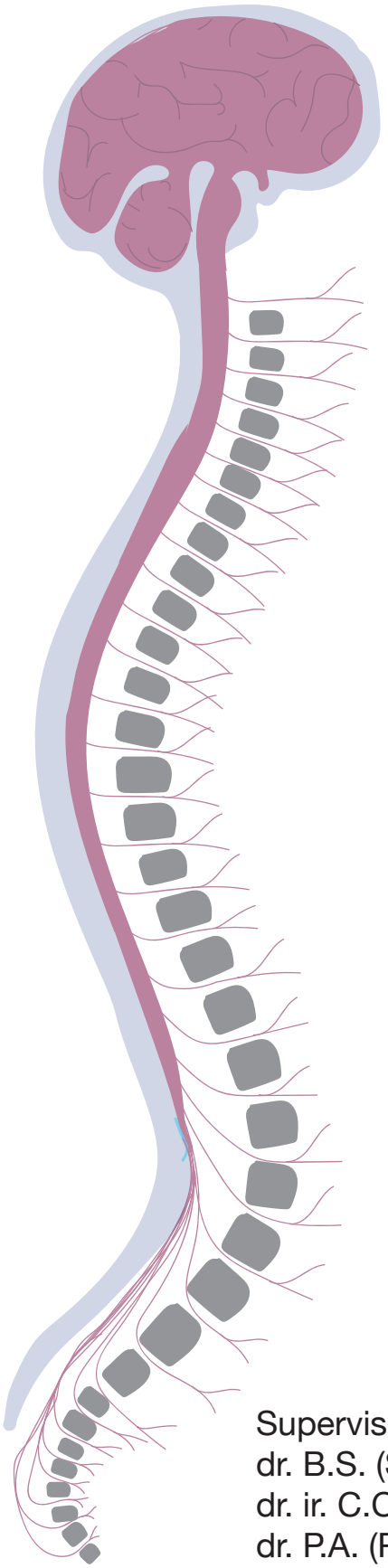

Master thesis

J. (Josephine) Dumas

TU Delft

Erasmus MC
Universitair Medisch Centrum Rotterdam

Supervised by
dr. B.S. (Sanjay) Harhangi
dr. ir. C.C. (Cecile) de Vos
dr. P.A. (Patrick) Forbes

Quantification of postural stability in the healthy population as reference for future research on Dorsal Root Ganglion stimulation in Spinal Cord Injury patients

by **J. (Josephine) Dumas**

Thesis in partial fulfillment of the requirements for the joint degree of Master of Science in

Technical Medicine

Leiden University | Technical University Delft | Erasmus University Rotterdam

Supervisors
Dr. B.S. (Sanjay) Harhangi
Dr. ir. C.C. (Cecile) de Vos
Dr. P.A. (Patrick) Forbes

Graduation committee
Prof. dr. ir. J. (Jaap) Harlaar (chair)
Dr. B.S. (Sanjay) Harhangi
Dr. ir. C.C. (Cecile) de Vos
Dr. P.A. (Patrick) Forbes
Dr. ir. J.J.M. (Johan) Pel

Department of Neurosurgery, Department of Neuroscience and Centre of Pain Medicine
Erasmus MC, Rotterdam

September 2020 - May 2021

Abstract

Introduction

Dorsal-Root-Ganglion (DRG) stimulation has been proposed as a neuromodulatory strategy in spinal cord injury (SCI) patients for the recovery of their impaired postural stability. A detailed evaluation of DRG stimulation-induced effects on postural stability can be obtained by recording center of pressure (CoP) and muscle activity during seated stability tasks, combined with the validated modified Functional Reach Test (mFRT). However, this particular combination of experiments has not yet been used to quantify postural stability in SCI patients or the healthy population. The aim of this study is to investigate postural stability in the healthy population utilizing a novel experimental protocol, involving this combination of experiments, to serve as reference for SCI patients in the upcoming long-term DRG stimulation study.

Methods

Twenty healthy volunteers participated in the experiments. CoP sway during upright sitting and multi-directional leaning was determined from force plate recordings. Furthermore, functional arm reach was assessed with the mFRT. Lastly, contribution of hip and trunk muscles was examined by retrieving muscle activation patterns and intermuscular coherence from surface electromyography (EMG) recordings during multi-directional trunk movements.

Results

During upright sitting an average root-mean-square CoP displacement of 1 mm, velocity of 4.5 mm/s and acceleration of 175 mm/s^2 was found. Maximum CoP displacements during multi-directional leaning were within 10 to 20 cm. Furthermore, the average functional arm reach was 50 cm in the forward direction and 30 cm in the lateral directions. The contribution of hip and trunk muscles to multi-directional trunk movements consisted of antagonist and contralateral muscle activation, accompanied by high intermuscular synchronization between 0-100 Hz for most neighboring muscle pairs.

Conclusion

This study provides a detailed examination of postural stability in the healthy population. Some revisions of the experimental protocol must be considered to reduce the amount of cross-registraton in EMG recordings. Nevertheless, the data of this study is well suited to be employed as reference for the potential improvements in postural stability in SCI patients during the upcoming long-term DRG stimulation study.

List of abbreviations

Abbreviation	Definition
AP	Anterior-ppsterior
BoS	Base of Support
CNS	Central Nervous System
CoM	Center of Mass
CoP	Center of Pressure
DRG	Dorsal Root Ganglion
ECG	Electrocardiography
EEG	Electroencephalography
EMG	Electromyography
GRF	Ground reaction force
mFRT	Modified Functional Reach Test
ML	Medial-lateral
RMS	Root-mean-square
SCI	Spinal Cord Injury
SENIAM	Surface ElectroMyoGraphy for the Non-Invasive Assessment of Muscles
TTL	Transistor-to-transistor logistic

Contents

1 Introduction

1.1 Postural stability in spinal cord injury patients

In the Netherlands, approximately 200 individuals suffer a traumatic spinal cord injury (SCI) each year.[1] A SCI is a devastating injury of the central nervous system (CNS) which could lead to loss of sensory and motor function, combined with bowel, bladder and sexual dysfunction, spasticity and chronic pain.[2] In thoracic or cervical SCI patients, the sensorimotor function loss can occur in the legs, hip and trunk, resulting in an impaired seated postural stability.[3] Postural stability can be divided into two components, static and dynamic. Static postural stability is the ability to keep the body in a sustained position, while dynamic postural stability is the ability to move the body in several directions without losing balance.[4]

For SCI patients, a decline in both static and dynamic postural stability can lead to a variety of problems. First of all, difficulties in maintaining an unsupported upright posture or performing unsupported trunk reaching tasks can substantially limit their independence in daily activities. Furthermore, to regain stability, SCI patients often employ compensatory strategies, which can lead to secondary health problems. Specifically, patients utilize non-postural muscles, e.g. upper-limb muscles, to compensate for the impaired trunk muscles[5,6] and tilt the pelvis backwards to increase their base of support.[7] This backward tilt often leads to a C-shaped kyphotic posture, which in the long term can cause breathing problems, back pain, pressure sores and skeletal deformities, including scoliosis when the SCI occured during childhood.[8,9] These secondary health problems combined with the impact on their independence, makes an improvement in static and dynamic postural stability one of the highest priorities for SCI patients.[2]

1.2 Physiology of postural stability

Human postural stability is maintained by a complex combination of interactions between sensory information and muscle action. These interactions are characterized by closed-loop feedback controlled by the CNS, consisting of the brain and spinal cord.[10] Figure 1 provides a simplification of the different interactions, roughly to be divided in two types of feedback loops. One loop resides in the spinal cord and is reliant on proprioceptive feedback, while the other loop resides in the brain and is reliant on the combination of proprioceptive, visual and vestibular feedback. The proprioceptive feedback consists of direct muscle feedback from the muscle spindles and Golgi's tendon organs (1) and movement feedback from joint mechanoreceptors and cutaneous receptors (2).[11,12] This proprioceptive information enters the dorsal root of the spinal cord via the dorsal root ganglion (DRG), whereafter the spinal reflex circuitry generates reactive motor output.[13,14] Furthermore, the brain processes the combination of vestibular, visual and proprioceptive information to generate supraspinal commands (3), which are send off to the spinal circuitry.[14] The interplay of these supraspinal commands and the feedback loops within the spinal circuitry is essential for maintaining postural stability. After a SCI however, the supraspinal commands are disrupted, while the spinal circuitry below the level of lesion is still intact. This intact spinal circuitry could serve as a potential target for motor rehabilitation, while bypassing the supraspinal commands.[15]

1.3 Interventions to improve postural stability in spinal cord injury patients

Rehabilitation programs often consist of an intensive in-house rehabilitation during the first months after injury, where patients are prepared for living with their disability at home. During this period, SCI patients are trained in wheelchair propulsion, performing transfers, participating in daily activities and preventing falling, all requiring sufficient static and dynamic postural stability. Furthermore, the wheelchair configuration is personalized in such a way that an optimal static seated stability is achieved, while aiming for adequate freedom in movements (dynamic stability) as well.

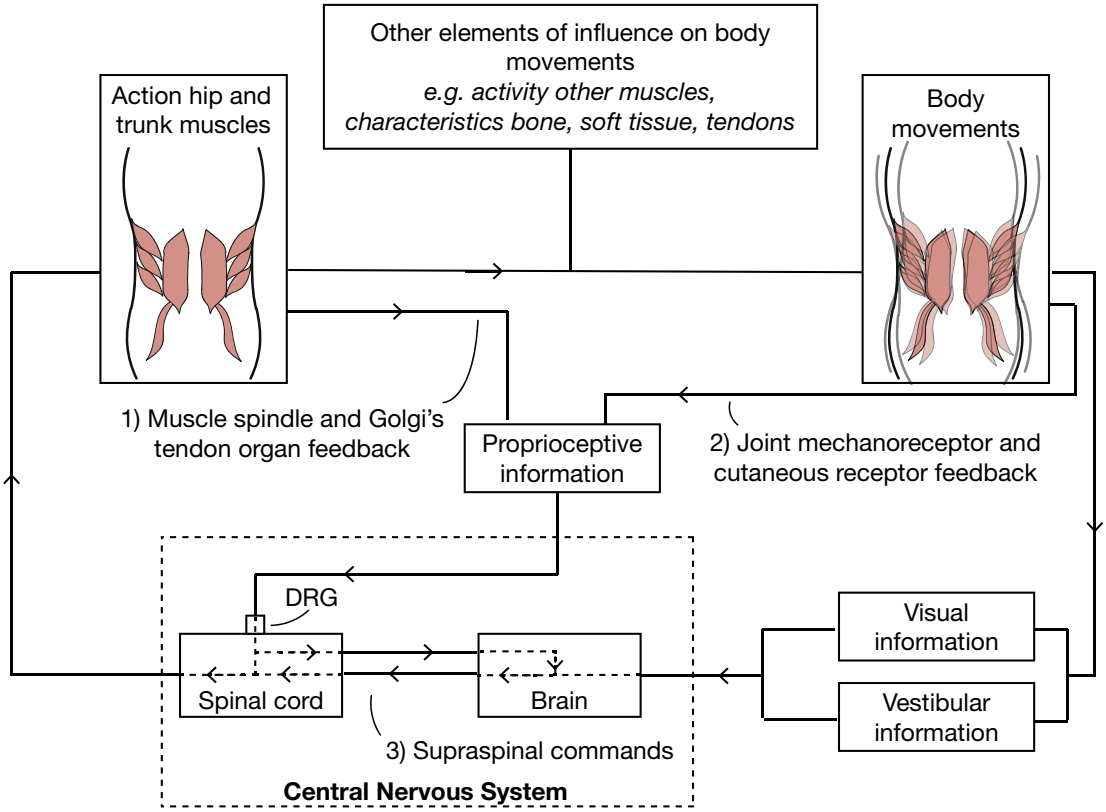

Figure 1: Interactions in the neuromuscular system all involved in maintaining postural stability. These include the direct muscle spindle feedback (1), movement feedback (2) and supraspinal commands (3). DRG = dorsal root ganglion.

Besides the conventional rehabilitation programs, novel approaches to specifically improve postural stability, even multiple years after injury, have been suggested. These approaches include specific stability exercise programs[5,16,17,18,19,20,21,22,23,24] or neuromodulation systems targeting the intact spinal circuitry below the level of lesion.[25,26,27,28,29] As an example of this latter approach, this upcoming year, a long-term safety and efficacy study on DRG stimulation in 10 motor-complete SCI patients will start. This type of neurostimulation, which is already an accepted therapy for chronic pain, involves placing electrode leads directly on the DRG's of specific spinal levels. Electrical stimulation is applied on the DRG's, which can potentially trigger the spinal circuitry to enhance muscle activation. In the pilot study published recently, where the activation of the knee extensor, m. Quadriceps, was targeted by placing the leads on level L4, three out of five patients reported an improvement of postural stability after a subthreshold stimulation period.[30] This feeling might be explained by the involvement of spinal level L4 and its surrounding spinal structures in the activation of not only the knee extensor, but also some trunk and hip muscles contributing to postural stability, including the lower back extensor m. Erector Spinae[31] and hip flexor m. Iliopsoas.[32] Therefore, exploring this effect of DRG stimulation motivated an objective evaluation of postural stability as a main study outcome for the upcoming long-term DRG-stimulation study.

1.4 Experimental protocol to quantify postural stability

To design a experimental protocol for quantifying the DRG stimulation effects on postural stability during the upcoming long-term DRG stimulation study, I conducted a literature review on postural stability quantification methods previously employed in SCI stability research.[33] Based on the findings in this review, we have decided to design a experimental protocol involving

1. the assessment of center of pressure (CoP) sway,
2. hip and trunk muscle electromyography (EMG),
3. and the evaluation of functional arm reach with the modified Functional Reach Test (mFRT).

We expect that this combination of measurements will be feasible to carry out in a clinical setting (e.g. no other rooms are needed besides a regular Clinical Neurophysiology examination room), and also will give us insight in different relevant interactions involved in postural stability. To elaborate, measuring CoP sway reflects the corrective trunk movements, muscle EMG measurements will give us insight in the action of the intact spinal circuitry below the level of lesion in generating motor output and the mFRT can reveal functional stability in the daily life setting.

1.4.1 Assessment of center of pressure sway

The measurement of center of pressure (CoP) displacements can be used to track the action of the human body to regulate the body's center of mass (CoM) within a base of support (BoS). For seated balance, the BoS is defined by the area of contact between the upper legs and buttocks with the support surface. Figure 2 visualizes the location of the CoP and the CoM in a simplified seated body in two non-static postures. The constant pull of gravity at the resultant CoM ($\sum$CoM, in green), which is the sum of the CoM of the two upper legs, lower legs and upper body,[34] requires continuous activity of the leg, hip and trunk muscles to prevent the body from falling.[35] The activity of muscles causes changes in the net forces into the support surface and the location of this ground reaction force (GRF) on the support surface is the CoP (in red). When the CoP and CoM are aligned and withing the BoS, the body will remain in quasistatic posture.[35] Movement of the CoP beyond the location of the CoM (as is the case in figure 2b and c), however, will accelerate the body in the opposite direction, whether this is to initiatie volitional movements or counteract unexpected disturbances of the CoM. Therefore, tracking the location of CoP over time is thought to give insight in this stabilizing action of the CNS.

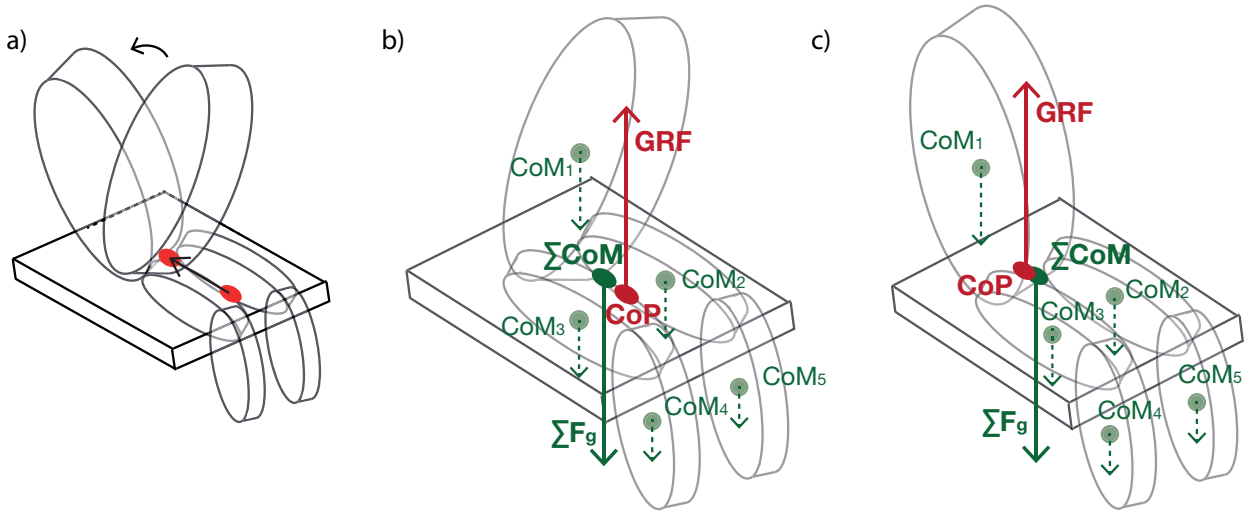

Figure 2: Center of pressure (CoP, red dots) and center of mass (CoM, green dots) during seated balance. a) The displacement of the CoP while changing trunk position in the anterior-posterior plane. b and c) Simplified seated balance model during two non-static trunk positions (leaning forward in b and leaning backward in c). $\sum$ CoM is the resultant of the center of mass (CoM) of the upper body, two lower and two upper legs. $\sum F_g$ is the resultant gravitational force acting on the $\sum$ CoM. The CoP is the location of the ground reaction force (GRF). The CoP is located beyond the $\sum$ CoM, which means that the body is accelerated in the opposite direction.

A force plate can be used to track the CoP displacements over time. A force plate measures the distribution of forces on its surface and expresses these in three resultant ground reaction forces and torques (Fx, Fy,Fz and Mx, My, Mz) acting at the center of the force plate. Figure 3 shows the directions of these forces and torques. The CoP location over time is calculated by assessing the medial-lateral (ML) coordinate (c_{ML}) and anterior-posterior (AP) coordinate (c_{AP}) from the force plate recordings, using

$$c_{\text{ML}} = M_{\text{y}}/F_{\text{z}} \quad \text{and} \tag{1}$$

$$c_{\text{AP}} = M_{\text{x}}/F_{\text{z}}\,. \tag{2}$$

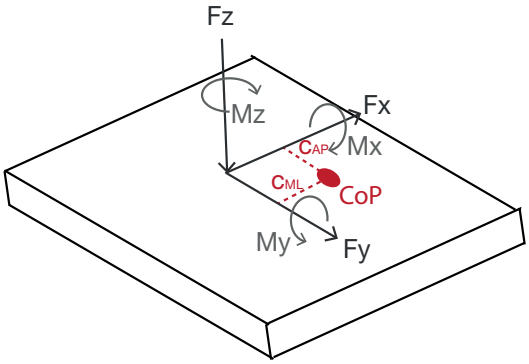

Figure 3: Direction of resultant ground reaction forces and torques as acquired by a force plate and the anterior-posterior (c_{AP}) and medial-lateral coordinates (c_{ML}) of the centre of pressure (CoP)

1.4.2 Hip and trunk muscle surface electromyography

Surface EMG is a way of measuring the electrical activation of muscles by recording the difference in electrical voltage between an active electrode, attached to the skin over the muscle of interest, and a reference electrode at electrically inactive tissue (e.g. bone). The electromyogram is a summation of all motor unit's end-plate potentials in the area between these two electrodes.[36] The down-fall of the signals acquired with surface EMG is that they are highly influenced by artifacts (e.g. movement, electrocardiography artifacts), noise, volume conduction through soft tissue (e.g. fat, skin) and cross-registration. Therefore, EMG signal amplitudes are highly dependent on electrode placement, environmental factors, body composition and filtering.[37] However, if performed correctly, the electromyogram serves as a good measure for muscle activation by the motor nerves.

1.4.3 Modified Functional Reach Test

The mFRT has been widely used in prior SCI stability research to assess functional stability.[17,18,24,21,19] The test originates from the Functional Reach Test, originally deployed to predict the risk of falling in elderly people. It has been modified for patients who are not able to stand, including motor-complete SCI patients.[38] The mFRT shows a test-retest reliability of more than 0.85[38] and a minimal detectable change of 4-5 cm,[19] making it suitable for the quantification of changes in functional stability over time.

1.5 Research objective

The simultaneous recording of CoP sway and muscle activity during seated stability tasks, in combination with the mFRT, can provide a detailed evaluation of DRG stimulation-induced effects on both static and dynamic postural stability in SCI patients. However, the proposed combination of experiments has never been done with SCI patients or healthy individuals. Accordingly, prior to evaluating postural stability of SCI patients using this protocol, a set of reference results needs to be gathered in a healthy population. Therefore, the aim of this research is to use the proposed measurements to gain insight in postural stability of the healthy population, as preparation on the interpretation of the similar acquired data in SCI patients during the long-term DRG stimulation study.

CoP sway and EMG will be recorded in healthy volunteers during two static tasks (sitting upright (1) and holding leaned positions (3)) and two dynamic tasks (maximum leaning (2) and moving the trunk in a circular motion (4, the sweep task)), which will be combined with one the mFRT (5). For comparison, three experiments will be done with one SCI patient, including the upright-sitting task (1), maximum leaning task (2) and mFRT (5). The experiments are aimed at answering the following research questions.

What is the CoP sway in a group of healthy volunteers and one SCI patient, when sitting upright (task 1) and during maximum leaning (task 2)?

What are the outcomes of the mFRT in a group of healthy volunteers and one SCI patient (task 5)?

How does the activity of trunk and hip muscles contribute to postural stability in a group of healthy volunteers during a static task, when holding the trunk in leaned positions (task 3), and during a dynamic task, when moving the trunk in a circular motion (task 4)?

2 Methods

2.1 Participants

Ten healthy male participants, ten healthy female participants and one 32-year-old female SCI patient with a motor-complete injury at spinal level T8 were included in this study. Table 1 provides an overview of participant characteristics. The average age of the healthy subjects was 38. For future comparison, both groups of healthy male and female subjects were matched on age with the group of ten SCI patients who participated in the pilot studies of the long-term DRG stimulation study.[30,39] For each matched pair, the age difference was chosen to be maximum three years.

Table 1: Participant characteristics

Healthy subject	**Age (years)**	**Gender (M/F)**	**Weight (kg)**	**Length (cm)**
1	56	M	68	175
2	23	M	67	180
3	53	M	85	182
4	27	M	87	188
5	27	M	70	180
6	24	M	70	188
7	49	M	79	189
8	37	M	67	175
9	34	M	82	184
10	50	M	90	190
11	32	F	67	176
12	25	F	58	158
13	23	F	63	172
14	38	F	53	168
15	24	F	61	178
16	50	F	58	162
17	56	F	84	165
18	52	F	74	172
19	52	F	70	170
20	26	F	63	173
SCI patient				
1	32	F	-	-

2.2 Experimental protocol

The experimental protocol consisted of five different seated stability tasks to examine static and dynamic postural stability. The assessment of static stability consisted of the sitting-upright task (task 1) and the hold-in-target task (task 3). Furthermore, dynamic stability was evaluated in the maximum leaning task (task 2) and sweep task (task 4) and functional reach was established in the mFRT (task 5). The SCI patient participated in three of the five tasks, including the sitting upright task, maximum leaning task and the mFRT, being test experiments at a time where the other two tasks were not yet included in the protocol. All tasks were performed with participants seated on a force plate (AMTI, USA). Participants were instructed to cross their arms in front of the chest and the seating surface was raised until feet were dangling for all tasks, except the mFRT. This was done to isolate the stabilization behavior to the trunk as much as possible.[23,25,40]

In figure 4 the measurement set-up is visualized to simultaneously acquire EMG and force plate during the tasks. The force plate was mounted on a height-adjustable seating surface. Since SCI patients are at high risk for developing decubitus wounds,[8] the force plate was covered with an anti-decubitus cushion. This cushion did not significantly affect the stability outcome measures, as seen in prior experiments.[41] Two beds were placed alongside the seating surface and a cushion was placed behind the force plate to provide support in the case participants would lose balance. EMG and force plate data were simultaneously collected and stored for offline analysis in an EMG cart at a sample frequency of 1000 Hz, using BrainRT electroencelography (EEG) software (OSG, Belgium).

Furthermore, the force plate data was, besides being collected in the EMG cart, also collected by the desktop via a data acquisition device (National Instruments, USA). On the desktop, a code was executed, written in Matlab software (Mathworks, USA), to derive real-time CoP coordinates from the force plate data using equations 1 and 2. The real-time CoP location was displayed on the screen as visual feedback for the participants during the maximum leaning, hold-in-target and sweep task. The start of measurements in each task was indicated by a countdown on the screen. Furthermore, at the start and end of measurements, a transistor-to-transistor logic (TTL) pulse was sent to the EMG cart to mark the timing of each task in the collected data.

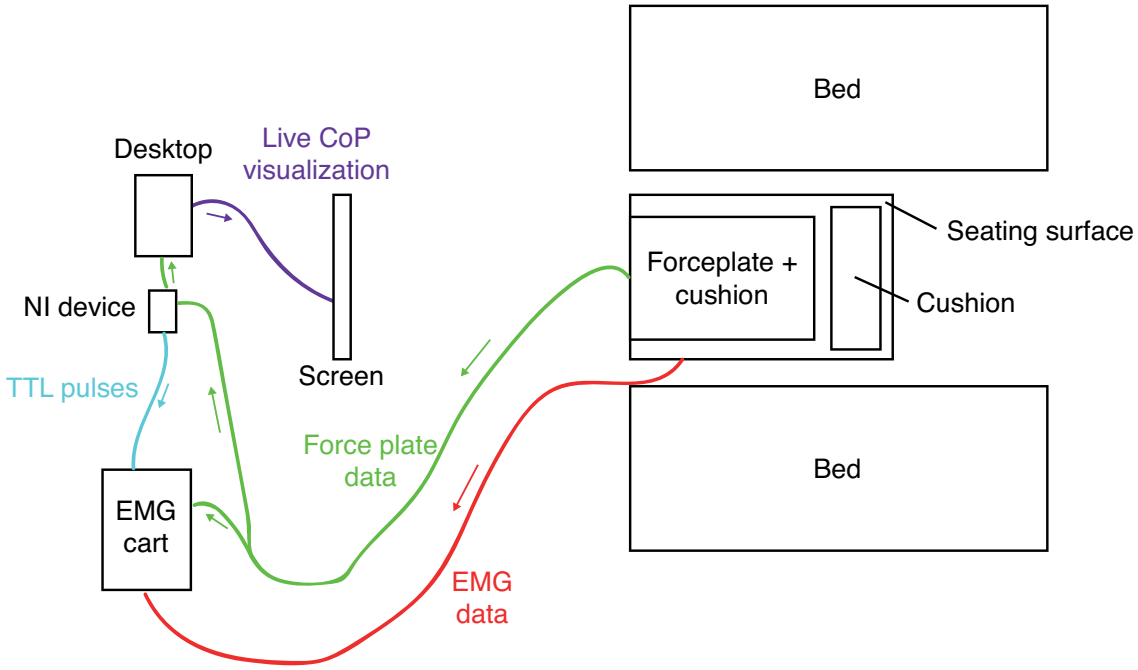

Figure 4: Measurement set-up and data flows. Electromyography (EMG, red data flow) and force plate (green data flow) data are collected in the EMG cart. The force plate data is also collected by the desktop via the National Instruments (NI) device, used to visualize real-time center of pressure (CoP) location feedback on the screen Transistor-to-transistor logic (TTL) pulses (blue data flow) are generated by the desktop and sent to the EMG cart to mark the start and end of each task.

Seated stability tasks

The upright-sitting task (task 1) was performed to evaluate static postural stability during an upright trunk posture. Participants were asked to sit upright for 30 seconds while focusing on a red dot on a screen. Trials were repeated three times.

Prior to the maximum leaning task, hold-in-target task and sweep task, participants were asked to sit upright for 10 seconds to estimate natural CoP variability, used to calculate their baseline area. Figure 6 shows this baseline area, serving as center of the real-time CoP visualization.

The maximum leaning task (task 2) was done to examine how far participants can lean in multiple directions without losing balance, an important aspect of dynamic postural stability. Participants were instructed to move their real-time CoP location in the indicated direction as far as they possibly could and then move back to their baseline area (figure 6a), as similar to experiments of Chisholm et al.[23] One trial consisted of eight directions being presented in random order, 45 degrees apart. Trials were repeated three times.

The hold-in-target task (task 3) was designed to assess muscle activation in static postural stability when holding leaning postures in multiple directions. Participants were instructed to move their real-time CoP location towards a red target (figure 6b). The target turned blue when the CoP was within the target. Participants were asked to maintain their CoP within the target for 30 seconds, where after the target turned green, being a cue for participants to move back towards baseline area. One trial consisted of eight targets being presented around the baseline area in random order, 45 degrees apart. The baseline-to-target distance was set to 0.5 times the mean of the maximum right lateral CoP displacement, as determined from the maximum leaning task. During testing, this choice for target location showed to result in a leaning position which needed some muscle effort, but was achievable to hold for 30 seconds. Moving towards the target and moving from the target to baseline was kept consistent by letting the participants count out loud till three during the leaning movements. Trials were repeated three times.

The sweep task (task 4) was performed to evaluate muscle activation in dynamic postural stability during a circular motion of the trunk. A circular moving target was visualized on the screen, and participants were instructed to follow the target while keeping the CoP location in between two circles (figure 6c). The baseline-to-target distance was the same as in the hold-in-target task. Participants were asked to follow the target for one-and-a-half rounds. Two trials of counter clockwise rotation and two trials of clockwise rotation were performed.

Functional arm reach was quantified using the mFRT (task 5). The seating surface was lowered until participants could use the ground as foot support to resemble daily life conditions. Participants were instructed to reach as far as possible with their arms stretched horizontally. This was repeated three times for reaching towards the right, towards the left and reaching forward. For the lateral reaches, participants were instructed to rest their non-reaching arm on their lap. For the forward reach, participants were instructed to reach with both arms. To keep height of both arms during forward reaching consistent, participants were given a straight pipe to hold with both hands. Figure 5 shows how the functional reach was measured. A ruler was placed on acromion height, and the position of the tip of the digitus medius (middle finger) was marked during upright sitting and after maximum reach. The functional reach was then defined as the difference between the two marks.

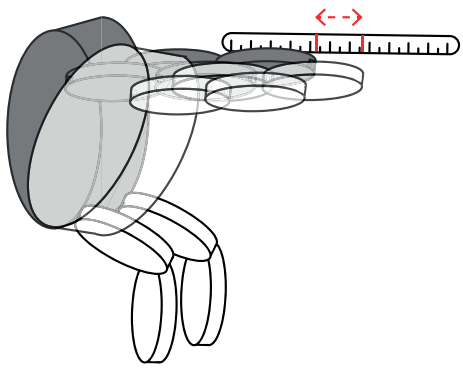

Figure 5: Modified Functional Reach Test (mFRT). Functional arm reach was defined as the difference between baseline and maximum reach position (red arrow).

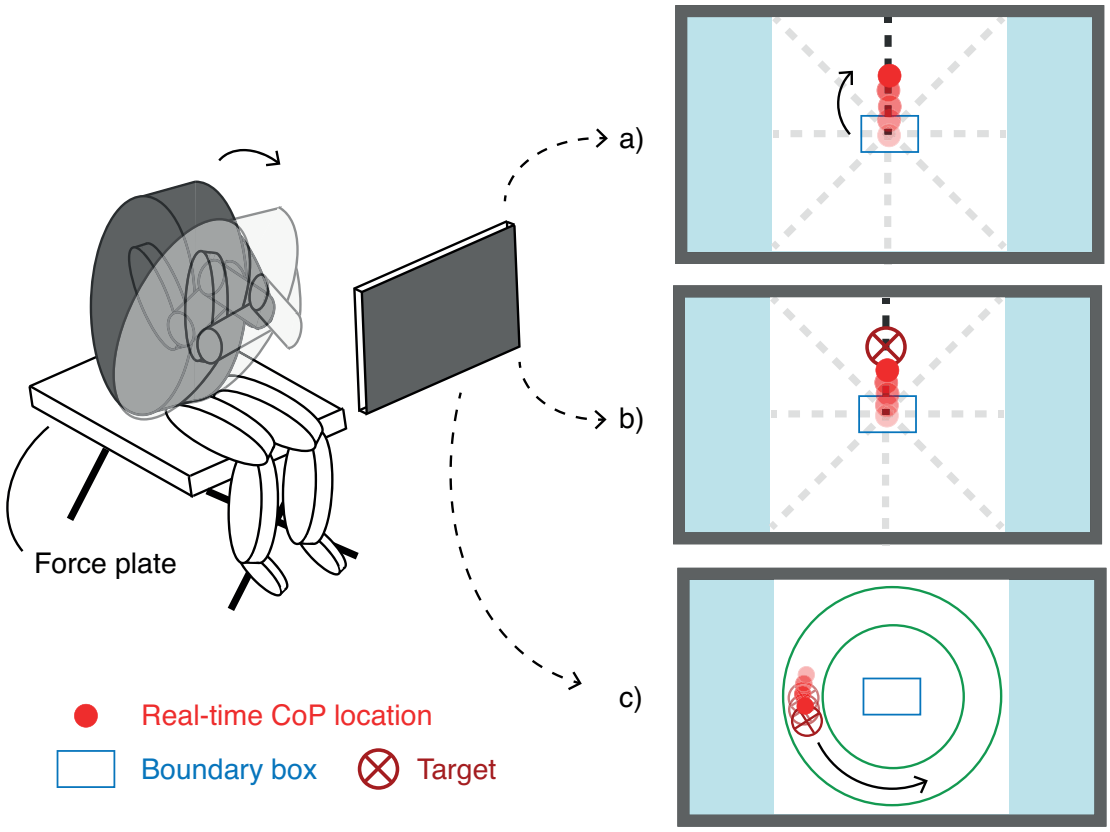

Figure 6: Visual center of pressure (CoP) location feedback during stability tasks. During the set-up period, where participants were asked to sit upright for 20 seconds, a baseline area (boundary box) was calculated. Thereafter, for the maximum leaning task in (a) and hold-in-target task (b), the leaning direction was showed on the screen (black dotted line) and the participant was asked to move the real-time CoP location over the dotted line. This was repeated for all eight directions (light grey dotted lines). For the sweep task (c), participants were asked to move the CoP location in a circular motion by following a moving target.

2.3 Recordings

During all tasks, besides the collection of force plate data, surface EMG was collected bilaterally from five trunk and hip muscles contributing to postural stability. Silver-silverchloride EMG electrodes were placed on the skin to bilaterally record activity from the m. Iliopsoas, m. Gluteus Maximus, m. Rectus Abdominis, m. Obliquus Externus and m. Erector Spinae at the level of the 3th lumbar vertebra. In figure 7, the anatomy of these muscles, as well as their function and innervation is shown. These muscles have been chosen for this study, since the innervation of all muscles is lower thoracic, lumbar and/or sacral thus might be impaired in SCI patients with a thoracic injury or lower. Furthermore, these muscles support in most trunk movements needed for the trunks range of motion. Placement of the surface EMG electrodes was based on the recommendations in the Anatomical Guide for the Electromyographer,[42] see appendix A for the detailed electrode locations.

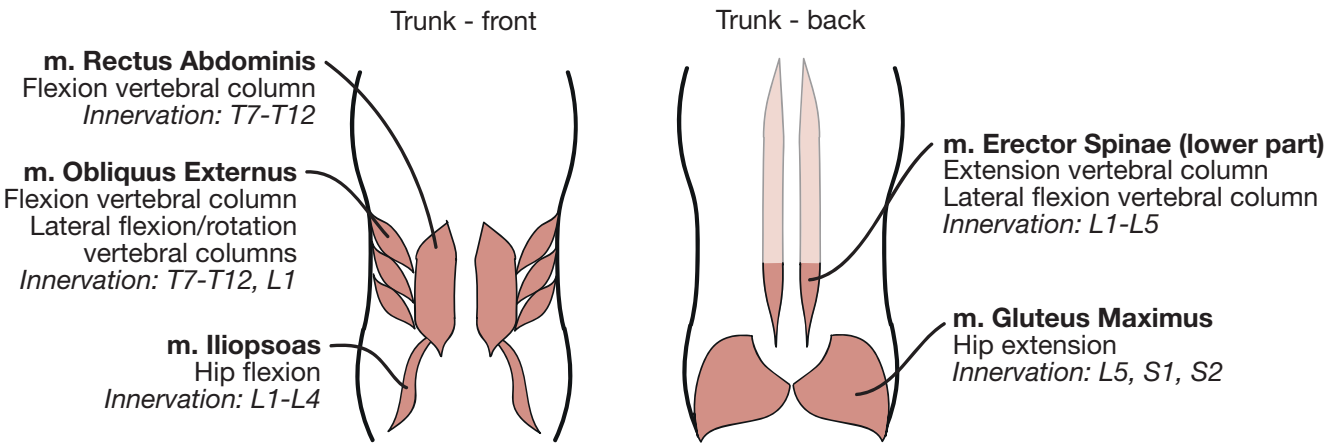

Figure 7: Trunk and hip muscles, which activity was recorded during the seated stability tasks. Left: the anatomy of abdominal trunk flexors (m. Rectus Abdominis and m. Obliquus Externus) and hip flexor (m. Iliopsoas) is shown. Right: the anatomy of the back extensor (m. Erector Spinae) and hip extensor (m. Gluteus Maximus) are shown. T = thoracic (spinal level), L = lumbar (spinal level), S = sacral (spinal level).

2.4 Signal analysis

Prepocessing

The raw data of all subjects was inspected and large artifacts were manually removed if possible. All data for subject no. 16 and the data during the maximum leaning task for subject no. 3 were so disturbed by large artifacts that manual removal was not possible. Therefore, this data was excluded from further analysis.

Force plate offsets were subtracted from the remaining data. Following, the three force outputs (F_{x}, F_{y} and F_{z}) and three torque outputs (M_{x}, M_{y} and M_{z}) were scaled to Newton and Newton-meter, respectively. Thereafter, the data was low-pass filtered using a 4$^{\mathrm{th}}$ order zero-phase 10 Hz low-pass Butterworth filter to remove electrical noise. A cut-off of 10 Hz was used in stead of the 5 Hz mostly used in previous research[43,44,45,46,47] so that still smaller, quicker signal changes could be captured. CoP coordinates were calculated from the filtered data for every time sample using equations 1 and 2.

The acquired EMG data for every bilateral muscle was filtered to get rid of movement artifacts, heartbeat artifacts and noise. Firstly, a notch of filter of 50 Hz and its harmonics was applied to eliminate electrical line noise. Thereafter, the data was band-pass filtered with a 8$^{\mathrm{th}}$ order zero-phase 30-400 Hz band-pass Butterworth filter. SENIAM recommends a band-pass filter with cut-offs of 20-400 Hz.[37] However, 30 Hz as high-pass cut-off seemed better suitable for the trunk muscles, as it succeeded more in suppressing the heartbeat artifacts, which yet dominated the signals with the recommended 20 Hz cut-off.

CoP sway during sitting upright and maximum leaning

CoP sway characteristics and maximum CoP displacements were calculated from the CoP coordinates during the upright-sitting task and maximum leaning tasks, respectively. The CoP coordinates were detrended by subtracting the average CoP coordinates during quiet sitting. Total displacement (CoP_{disp}) during both tasks was calculated using

$$CoP_{\mathrm{disp}} = \sqrt{c_{\mathrm{ML}}^2 + c_{\mathrm{AP}}^2}), \tag{3}$$

where c_{ML} and c_{AP} are the ML CoP coordinate and AP CoP coordinate respectively. The first 5 and last 1 seconds were removed from every trial of the upright-sitting task, so that 24 seconds remained. Root-mean-square (RMS) displacement (RMS_{disp}), velocity (RMS_{vel}) and acceleration (RMS_{acc}) were retrieved from the CoP_{disp} using

$$RMS_{\text{disp}} = \frac{1}{N}\sum_{n=0}^{N} CoP_{\text{disp}}[\text{n}]^2, \tag{4}$$

$$RMS_{\text{vel}} = \frac{1}{N}\sum_{n=0}^{N} CoP_{\text{vel}}[\text{n}]^2, \qquad \text{where } CoP_{\text{vel}}[\text{n}] = \Delta CoP_{\text{disp}}[\text{n}]\text{and} \tag{5}$$

$$RMS_{\text{acc}} = \frac{1}{N}\sum_{n=0}^{N} CoP_{\text{acc}}[\text{n}]^2, \qquad \text{where } CoP_{\text{acc}}[\text{n}] = \Delta CoP_{\text{vel}}[\text{n}]. \tag{6}$$

In these equations, N is the total number of samples in each trial. The maximum CoP displacements for all eight directions during the maximum leaning task were retrieved by taking the maximum of the CoP_{disp}.
For every subject, the RMS_{disp}, RMS_{vel}, RMS_{acc} and maximum CoP displacements, as well as the functional reaches from the mFRT, were averaged over the three trials. Thereafter, group average, standard deviation and 95% confidence interval of all outcome measures were calculated for male, female and all subjects. Furthermore, to relate the outcome measures to participant characteristics, including total height, weight and age, Pearson correlation coefficients were calculated.[48] The relation between the maximum CoP displacements during the maximum leaning task and the functional arm reaches during the mFRT was also assessed by calculating Pearson correlation coefficients.

Muscle activation patterns

Multi-directional muscle activation patterns during the hold-in-target task and sweep task were retrieved from the filtered EMG recordings. CoP coordinates were used to mark the start and end of each leaning position and sweep. For the hold-in-target task, the start of each leaning position was defined as the moment where the CoP total displacement was at its maximum and the end was defined 30 seconds after the start. The first five seconds and last one second of each segment was cut, so that 24 seconds of data remained per leaning position. Over each segment of 24 seconds, the RMS EMG value of each muscle was computed. To generate normalized activation patterns which are comparable between muscles, per direction the EMG RMS values were normalized by the muscle's maximum RMS EMG value of the whole trial (including all directions). For every subject, the resulting RMS EMG values for every direction were averaged over the three trials, where after a group average was calculated.

For the sweep task, the start of one circle was defined as the moment where the CoP coordinates were at the most left position for the counter-clockwise sweep and at the most right position for the clockwise sweep. The end of each sweep was defined at 43 seconds after the start. Between start and end, the EMG data of all muscles was rectified and low-pass filtered with a 4$^{\text{th}}$ order zero-phase 2 Hz low-pass Butterworth filter, to create smooth EMG envelops for visualization.[49] Per trial the EMG envelop of each muscle was normalized by the muscle's maximum EMG envelop value in that same trial. For every subject, the resulting EMG envelops were averaged over the two trials per direction (counter-clockwise and clockwise), whereafter a group average was calculated.

EMG-EMG intermuscular coherence

EMG-EMG intermuscular coherence during the sweep task was obtained to examine muscle synchronization within the hip and trunk muscles. Prior to coherence analysis, the EMG signals for every sweep trial were full-wave rectified, which is often recommended for intermuscular coherence since common spinal input might be reflected in EMG amplitude fluctuations.[50] Coherence was calculated with a multi-taper method using the open-source NeuroSpec toolbox (version 2.1, by Halliday[51]). Tapers were based on the Slepian sequences, where each taper is orthogonal to all other tapers and thus statistically independent.[52] Hence, since coherence is estimated by averaging multiple independent tapered segments, this multi-taper method generally results in lower estimation bias compared to other averaging methods.[53] The rectified signals were broken down in 42 segments with sample length of 1024 (2^{10}) samples. 11 tapers were multiplied with the segments, where after the independent Fourier transform cross spectra for all segments were calculated. The recommended number of tapers depends on the number of samples per segment and frequency bandwith of interest.[54] Both are quite high for this analysis (1024 samples per segment and 0-100 Hz as frequencies of interest), which is the reason why the maximum number of 11 tapers was chosen. The acquired cross spectra were averaged over all tapered segments and the averaged spectra were used to calculate the coherence estimate for each muscle pair (see section 5 of Halliday et al.[55] for formulas used). Furthermore, per sweep trial a 95% confidence limit for coherence was calculated, which was corrected for the number of tapers used. For each subject, the estimated cross-spectra and 95% confidence limits were averaged over the two sweep trials per direction (counter-clockwise and clockwise) and a group average was calculated.

3 Results

3.1 CoP sway during upright sitting

During upright sitting (task 1), CoP displacement of the healthy subjects was generally kept within a few mm, accompanied by a CoP velocity of multiple mm/s and an acceleration of multiple cm/s^2. Figure 8a shows the CoP sway during one trial of 30 seconds, characterized by micro-oscllations around the center. Furthermore, figure 8b shows the group average of the RMS CoP displacement (1.0 mm), velocity (4.5 mm/s) and acceleration (175 mm/s^2). As indicated by the 95% confidence intervals, higher relative inter-subject variability was seen in CoP velocity and acceleration, when compared to CoP displacement. Notably, the group of female subjects showed lower displacements, velocity and acceleration compared to the male subjects. Table 3 in appendix B provides the individual CoP sway characteristics of all participants. All Pearson correlation coefficients between participants characteristics (age, weight and height) and CoP sway characteristics were defined as negligible or low, since none exceeded 0.5. Appendix E provides all correlation coefficients.

The SCI patient showed a CoP sway with higher displacement (1.6 mm), lower velocity (3.5 mm/s) and lower acceleration (77 mm/s^2) compared to the healthy subjects (figure 8b and table 3 in appendix B).

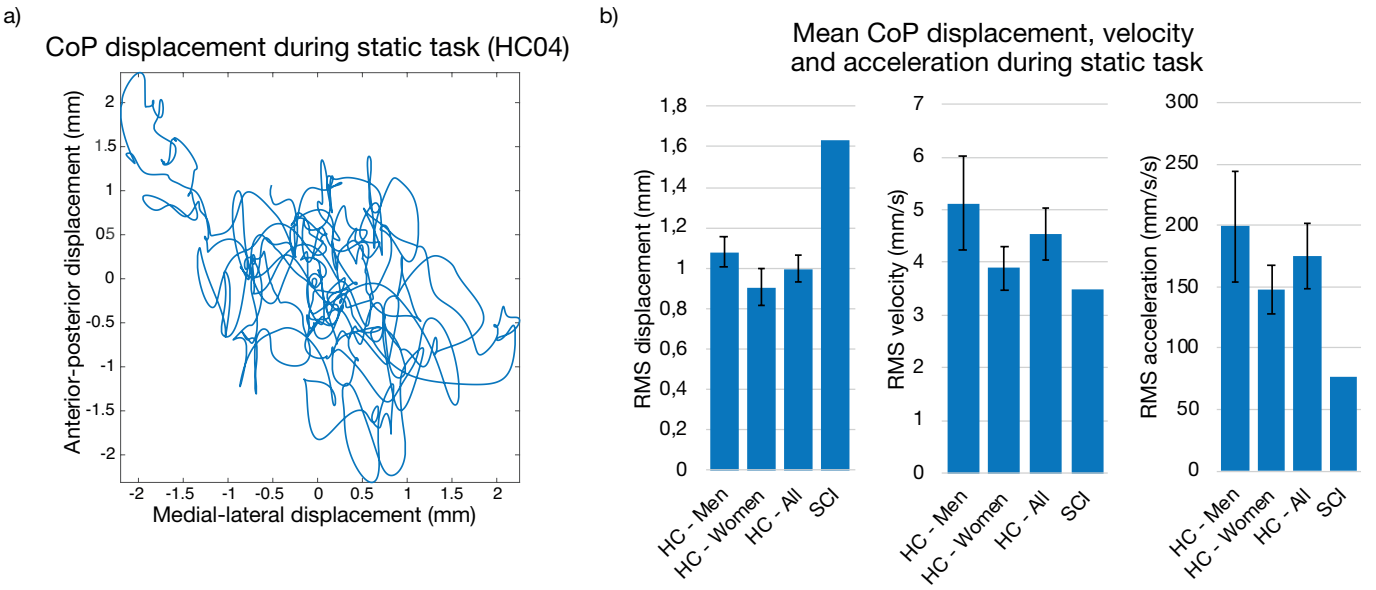

Figure 8: Center of pressure (CoP) displacement during the static sitting-upright task. a) CoP displacement for healthy subject no. 4 (HC04) during one full trial of 30 seconds. b) Group average of the root-mean-square (RMS) CoP displacement, velocity and acceleration for the male (HC - Men), female (HC - Women), all (HC - All) healthy subjects and the spinal cord injury patient (SCI). The inter-subject variability is indicated by the error bars representing 95% confidence intervals.

3.2 CoP displacement during maximum leaning

During the maximum leaning task (task 2), the healthy subjects were generally able to move their CoP location within 10 to 20 cm in the indicated directions. Figure 9a shows the CoP sway during a full trial of one healthy subject, including all eight directions. Figure 9c reveals the average maximum displacements for the eight directions. For the male subjects, maximum displacement was highest for forward leaning directions (N, NE, and NW) and lowest for lateral leaning (E and W), which was not the case for the female subjects, since they showed relatively lower maximum displacements for the forward directions (N, NE and NW). As indicated by the

95 % confidence intervals in figure 9, a notably higher inter-subject variability for the leaning directions N and S, compared to the lateral leaning directions E and W was seen. Table 4 in appendix C shows the individual maximum displacements of all participants. Most Pearson correlation coefficients between participants characteristics (age, weight and height) and maximum displacements were defined as negligible or low, since none exceeded 0.5, except for the correlation between weight and maximum displacement in the S direction, which was 0.52 and defined as moderate (appendix E).

The SCI patient showed substantially lower maximum displacements in all directions compared to the healthy subjects, as seen in figure 9c and table 4 in appendix C. Furthermore, figure 9b visualizes the CoP trajectory during one full maximum leaning trial of the SCI patient, which deviated more from the target trajectory as compared to healthy subject no. 6 in figure 9a.

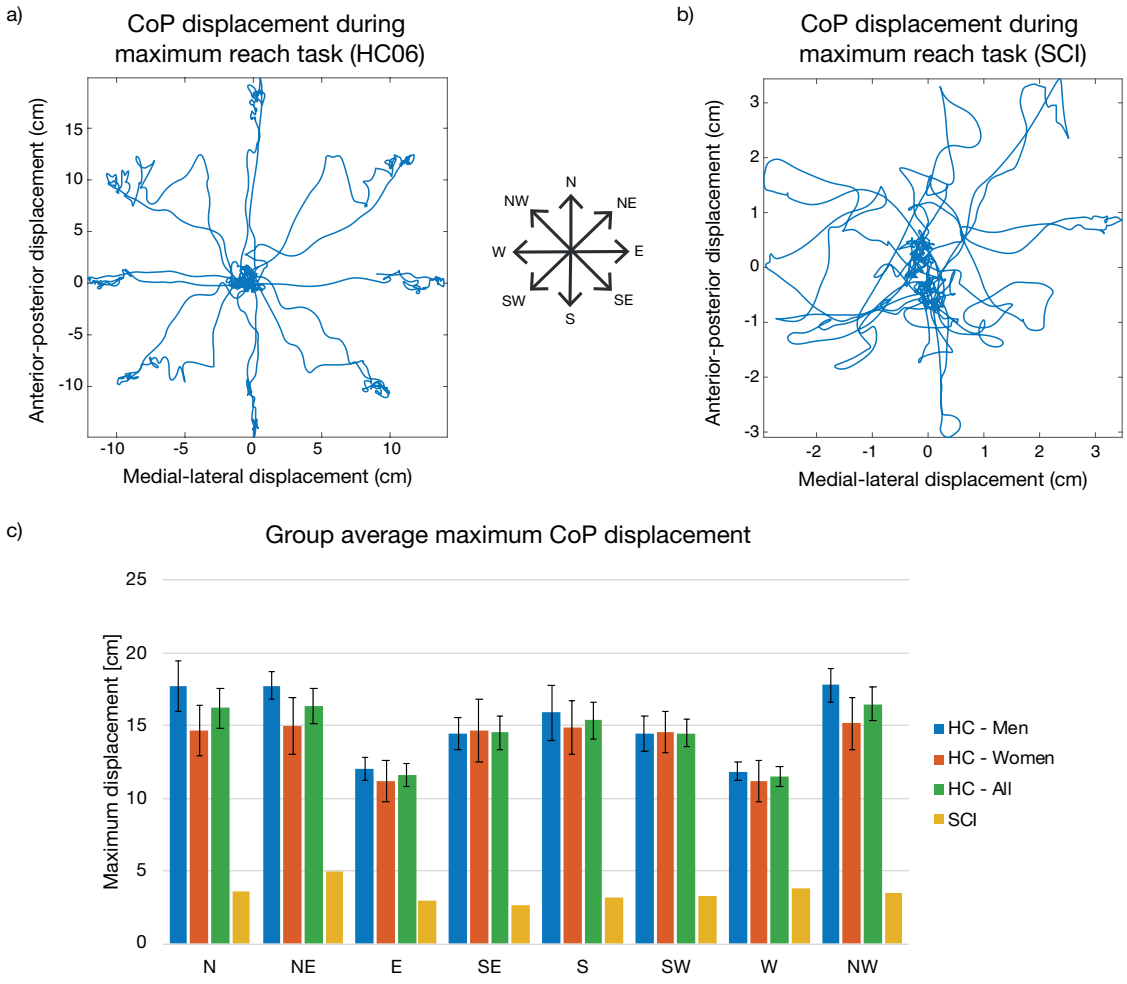

Figure 9: Maximum center of pressure (CoP) displacement during the maximum leaning task in eight directions. a) the CoP displacement for healthy subject no. 6 (HC6) during one full trial. b) CoP displacement for the spinal cord injury patient (SCI) during one trial. c) Group average of maximum CoP displacement in the eight directions for the male (HC - Men) female (HC - Women) and all healthy subjects (HC - All), and maximum CoP displacement for the SCI patient. The inter-subject variability is indicated by the error bars representing 95% confidence intervals. N = North, NE = North-East, E = East, SE = South-East, S = South, SW = South-West, W = West, NW = North-West.

3.3 Modified Functional Reach Test

During the mFRT, healthy subjects achieved functional forward reaching distances of 50 cm, and functional lateral reaching distances of 30 cm, as seen in figure 10a. Table 5 in appendix D provides an overview of all individual results. All Pearson correlation coefficients between participants characteristics (age, weight and height) and functional reaching distances were defined as negligible, since none exceeded 0.3 (appendix E). Furthermore, figure 10b shows the the Pearson correlation coefficients between the functional arm reaches from the mFRT and the maximum CoP displacements from the maximum leaning task in the directions the two tasks shared. Since no coefficient exceeds the 0.3, also these are defined as negligible or low.

The SCI patient achieved reaching distances of 11, 17 and 22 cm in the forward, left and right direction respectively, which are smaller compared to the healthy subjects. Furthermore, the SCI patient showed smallest reach distance in the forward direction, while for the healthy group this direction resulted in largest reaching distances.

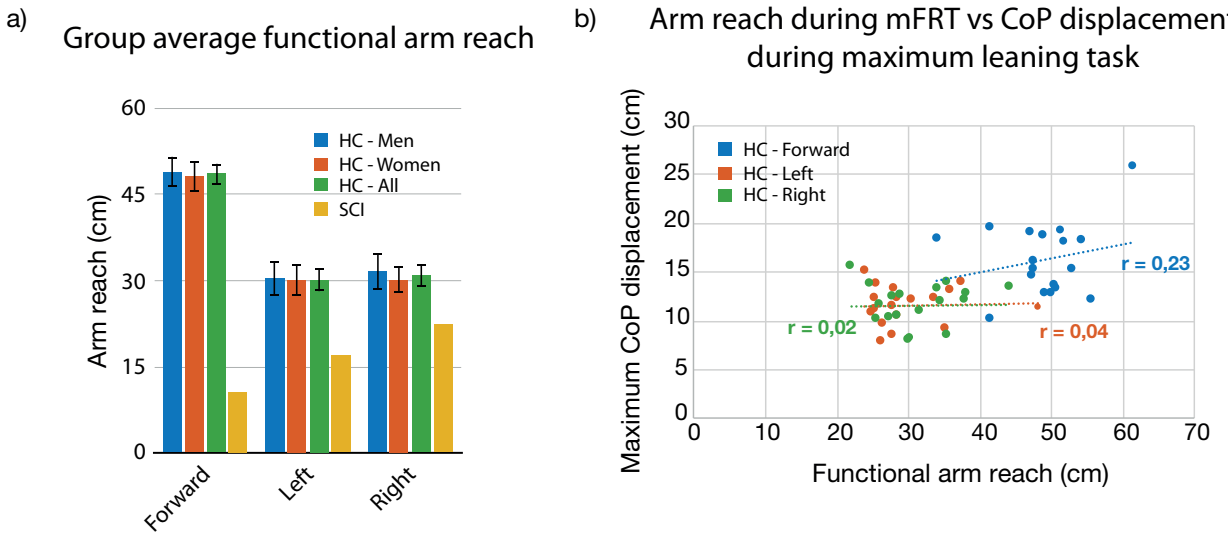

Figure 10: Functional arm reach during the modified Functional Reach Test (mFRT). a) Group average for forward, left and right reach for the male (HC - Men), female (HC - Women) and all healthy subjects (HC - All), with error bars indicating the 95% confidence intervals, and the arm reaches of the spinal cord injury patient (SCI). b) Scatter plot of all healthy subjects (HC) to display relation between functional arm reach in the mFRT and the maximum CoP displacement in the maximum leaning task (see figure 9) for forward, left and right reach (corresponding with North, West and East directions in the maximum leaning task), with Pearson correlation coefficients (r).

3.4 Muscle activation when holding leaned postures

Figure 11 shows the activity of all muscles during the hold-in-target task. The RMS EMG amplitudes reveal antagonist activation patterns for most muscles, meaning that muscles were most active in the direction which is opposite of their function (e.g. the m. Erector Spinae is most active during forward flexion, while its function is to extend the trunk). The back extensor, m. Erector Spinae, was particularly active during forward leaning, while the two abdominal muscles (m. Rectus Abdominis and Obliquus Externus) were most active in backward leaning postures. Furthermore, the hip flexor, m. Iliopsoas, was most active during backward and lateral leaning. The hip extensor, m. Gluteus Maximus, did not show this particular antagonist activation pattern, since its activation pattern was more uniformly distributed over the directions and even showed a trend towards agonist activity, with the muscle most active during backward leaning. Furthermore, all muscles activation patterns were defined by contralateral activation, meaning that each muscle was more active when leaning to the contralateral compared

to the ipsilateral direction (e.g. the left muscles are more active during leaning to the right than during leaning to the left).

3.5 Muscle activation during a circular trunk movement

Muscle activation patterns

EMG amplitudes of most muscles during the dynamic sweep task (task 4) showed similar contralateral and antagonist muscle activation patterns as during the static leaning postures in the hold in target task. Figure 12 shows CoP displacement and muscle activity during the circular movement covering one and a half counter-clockwise circle. The back extensor, m. Erector Spinae, was most active over the anterior half of the circular movement, while the abdominal muscles, m. Rectus Abdominis and m. Obliquus Externus, were particularly active in the posterior half. Furthermore, the hip flexor, m. Iliopsoas, was most active in the posterior and lateral parts of the circular movement. As similar as during the leaning postures in the hold-in-target task, the m. Gluteus Maximus showed a more uniformly distributed and agonist activation pattern. Furthermore, contralateral activation patterns were seen for all muscles, indicated by the difference in activation between the left and right muscles.

Intermuscular coherence

The assessment of intermuscular EMG-EMG coherence during the counter-clockwise circular trunk movement in the sweep task (task 4) resulted in high coherence between most right muscle pairs over a broad frequency spectrum, as seen in figure 13. Only in three muscle combinations no significant coherence was seen, all involving the back extensor, m. Erector Spinae. This muscle solely showed high coherence with the hip extensor, m. Gluteus Maximus, at frequencies up to 50 Hz. Furthermore, coherence was most prominent between the two agonist abdominal muscles, m. Rectus Abdominus and m. Obliquus Externus. Both trunk flexors also showed high coherence with their hip agonist muscle, m. Iliopsoas and with their hip antagonist, m. Gluteus Maximus. Likewise, the pair of antagonist hip muscles (m. Gluteus Maximus and m. Iliopsoas) showed high and statistical significant coherence.

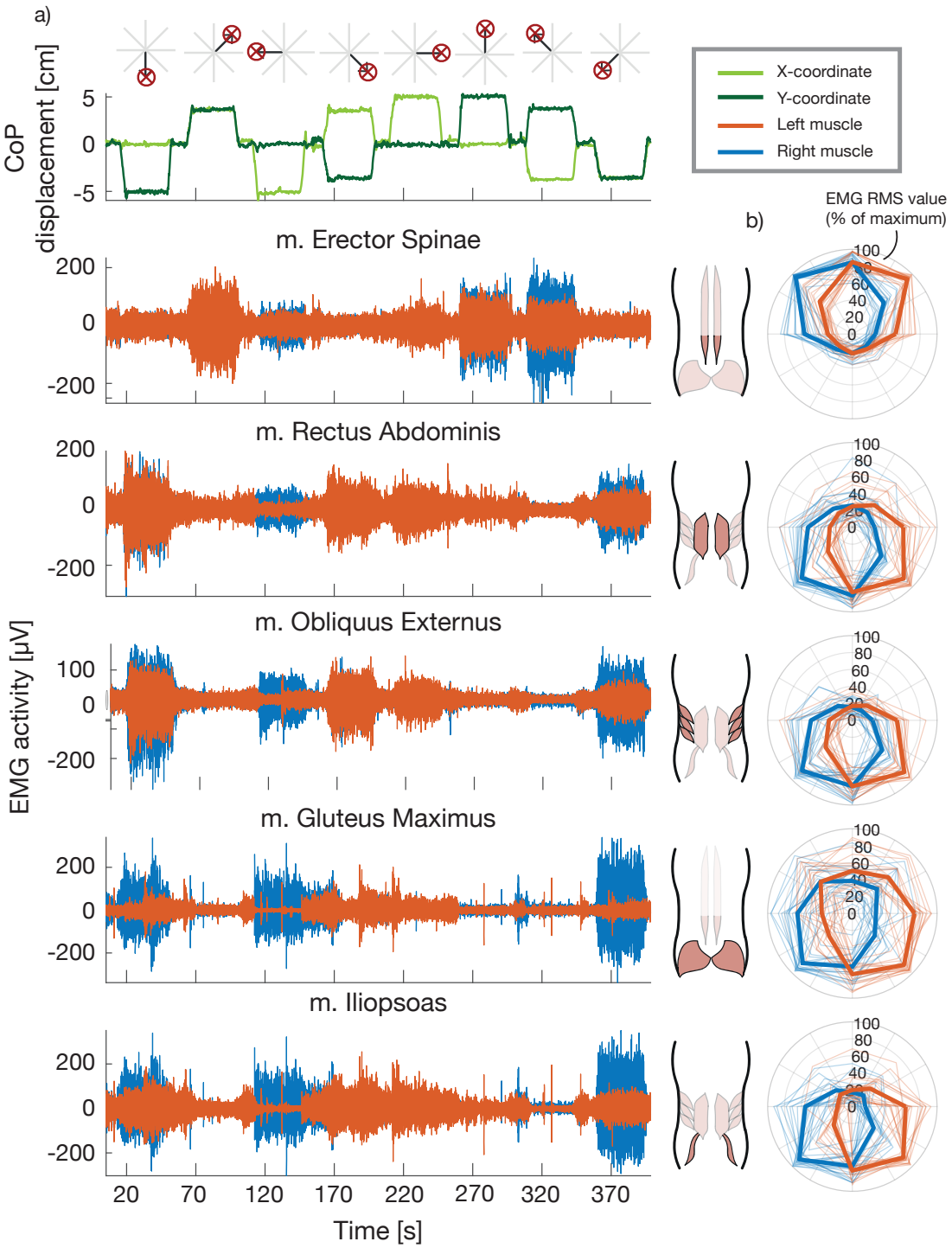

Figure 11: Muscle EMG activity during hold-in-target. a) Center of pressure (CoP) displacement and electromyography (EMG) activity of the five bilateral trunk and hip muscles during one full run of the target task. b) Root-mean-square (RMS) muscle activity of the leaning postures in eight directions. The shaded lines represent the RMS EMG values of individual participants, normalized to the maximum value, and the bold line represents the group average.

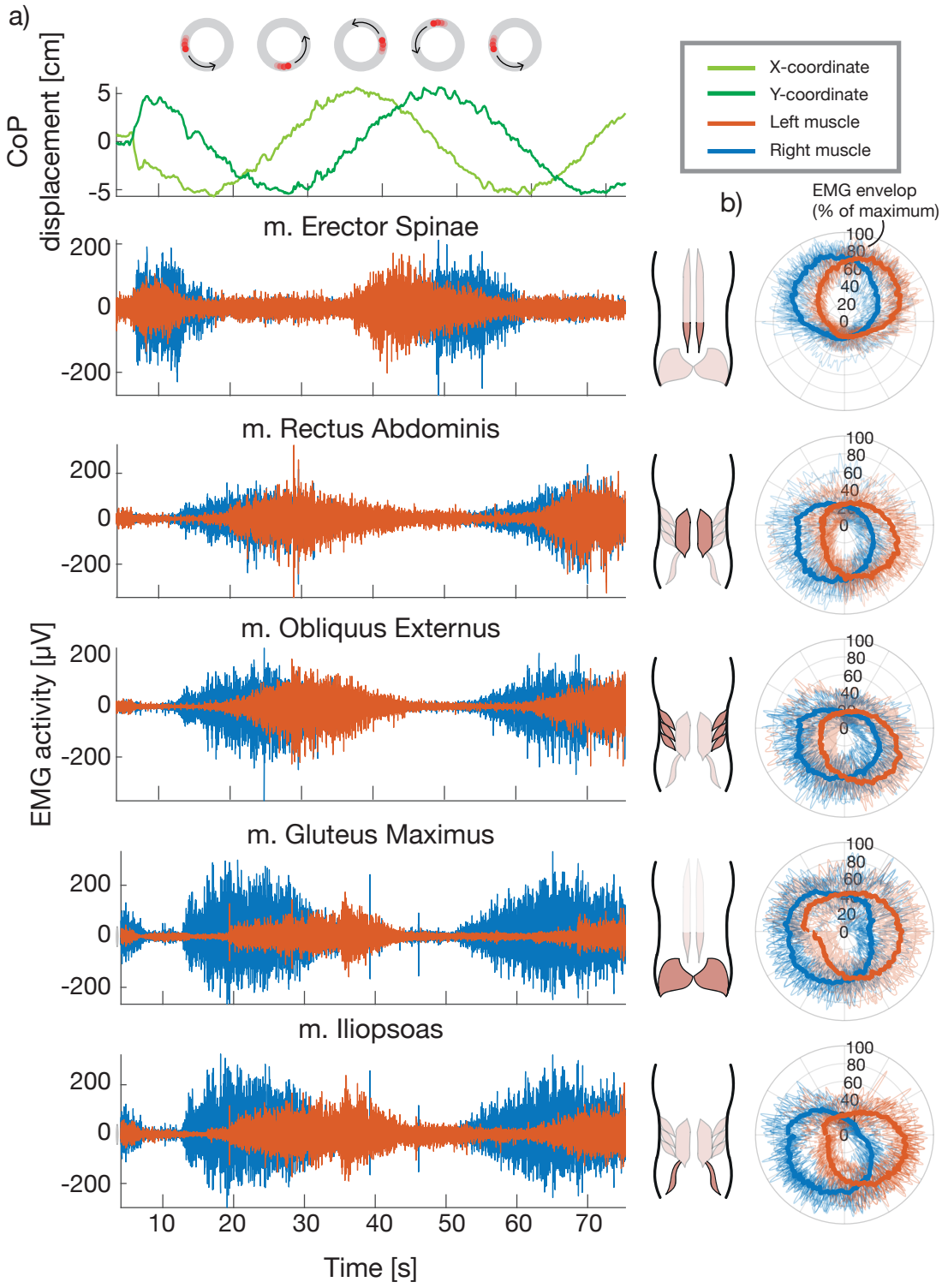

Figure 12: Muscle activity during counter-clockwise sweep. a) Center of pressure (CoP) displacement and electromyography (EMG) activity of the five bilateral trunk and hip muscles during one and a half sweep (HC05). b) Group average of muscle activity displayed in a polarplot, representing the circle travelled during the counter-clock wise sweep task. The shaded lines represent the EMG envelops of individual participants, normalized to the maximum EMG value, and the bold line represents the group average.

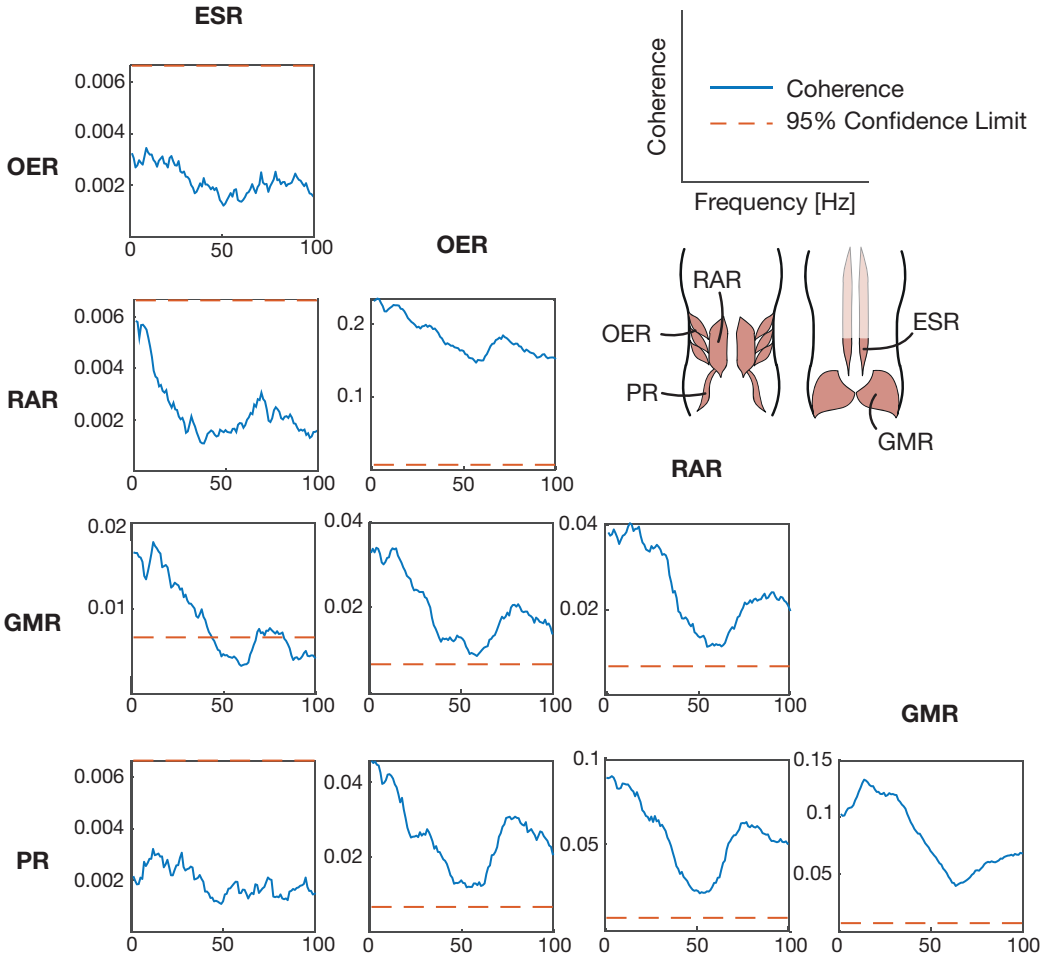

Figure 13: Group average of intermuscular coherence of all combinations of the five right muscles during one counter-clockwise circular trunk movement. The blue line represents the coherence. The limit of significant coherence is indicated by the orange dotted line, representing the 95% confidence limit. ESR = right m. Erector Spinae, OER = right m. Obliquus Externus, RAR = right m. Rectus Abdominis, GMR = right m. Gluteus Maximus, PR = right m. Iliopsoas

4 Discussion

This study explored static and dynamic seated postural stability in healthy individuals and one SCI patient using a novel measurement protocol, which is proposed for the future assessment of DRG stimulation effects in SCI patients. Our results showed an enhanced static and dynamic stability in healthy individuals compared with the SCI patient, as identified by smaller and quicker corrective displacements during static upright sitting and the capability to reach and lean further. Furthermore, the contribution of hip and trunk muscles to multi-directional trunk movements consisted of antagonist and contralateral muscle activation, accompanied by high intermuscular synchronization between 0-100 Hz for most neighboring muscle pairs.

4.1 CoP sway characteristics during upright sitting

The RMS CoP displacement of 1 mm and velocity of 5 mm/s recorded in the healthy subjects during upright sitting are similar to those found in other research.[43,44] Although no previous research reported CoP acceleration in healthy subjects, CoP accelerations in SCI patients had been reported between 1-4 m/s^2 by Rath et al.[25] This, however, remains well above the CoP acceleration we recorded with 17 cm/s^2 for the healthy subjects and 7 cm/s^2 for the SCI patient. This large difference may be due to inter-subject variability, as Rath et al. had reported a large standard deviation of 3 m/s^2. However, their lower choice of sample rate (50 Hz versus 1000 Hz here), might have missed subtle CoP displacements, resulting in an overestimated acceleration. Moreover, where previous research proved that assessing RMS CoP displacement could distinguish subjects with impaired stability from healthy subjects,[43,45,46] no significant differences have been found for velocity[43,45] and acceleration outcome measures when comparing healthy individuals and those with impaired stability. These previous findings, combined with the inconsistency in CoP acceleration between studies, indicate that the RMS CoP displacement results are, but velocity and acceleration results might not be suitable for the objective quantification of postural stability.

4.2 Maximum CoP displacements during leaning

For the healthy subjects, the recorded maximum displacements during forward (16 cm) and backward (15 cm) leaning were larger than the 13 and 12 cm previously reported by Kerr et al„ while the displacements for the lateral directions were comparable.[56] The participants of Kerr et al. were seated on the force plate with 80% of thigh length on the plate, whereas our participants utilized 100% of thigh length, increasing the base of support (BoS). Since CoP displacement is naturally limited by the BoS, this difference in anterior-posterior BoS size might explain the ability of our participants to move the CoP further in the forward an backward direction. However, Preuss et al. revealed that healthy subjects were not able to move their CoP to the BoS outer edges, but only reached CoP displacements of 70% BoS length in anterior-posterior direction and 50% BoS width in medial-lateral direction.[57] Therefore, other aspects than BoS dimensions alone define inter-subject variability of maximum CoP displacements.

Since individuals move their CoP by applying forces to the seating surface, muscle activation and strength are further determining factors for maximum CoP displacement. This explains the fact that the SCI patient in our study, who lacks muscle activation below the level of her lesion (T8), achieved four-fold smaller maximum CoP displacements than the healthy subjects, while having similar BoS dimensions. Maximum CoP displacements of 3-5 cm for the SCI patient were recorded, which is comparable to previously reported forward leaning CoP displacements of 2-4 cm in thoracic SCI patients.[58,59] However, a total sum of 20-25 cm was reported in three SCI patients with injuries at the level of C7, T3 and T4,[23] which is slightly lower than the total of 28 cm (sum of all eight directions) found here. This difference may be explained by our SCI patient suffering an injury at a lower spinal level (T8) and therefore having more residual motor function to move the CoP further in the indicated directions.

4.3 Functional arm reaches during the modified Functional Reach test

The average functional arm reaches of the healthy subjects during the modified Functional Reach Test (mFRT) were in the range of 50 cm when reaching forward and 30 cm for the lateral directions. These values are larger compared to Singh et al., who found a functional forward arm reach of 38 cm and 25 cm and lateral reach of 18 and 14 cm in a young (20-40 years) and old (40-60) group of healthy individuals, respectively.[60] This difference might be explained by variability in anthropomorphic characteristics between the two populations. As we did not find correlations between functional arm reach and participants characteristics, including total height, weight and age, Singh et al. did find a significant positive correlation between trunk length and reach.[60] We did not account for this specific characteristic, however, it might have been larger for our subjects, since their average total height (175 cm) was also higher than the 162 cm in the subjects of Singh et al.[60]

The average functional forward reach of the SCI patient of 11 cm was lower than forward reaches reported elsewhere in SCI patients. However, mFRT results are highly dependent on injury characteristics, including the completeness and level of injury, both determining the amount of residual motor function in the trunk and upper body. For example, motor-incomplete SCI patients have been reported to reach further compared to motor-complete SCI patients, with a functional forward reach of 48 and 23 cm, respectively.[17] Moreover, a significantly larger forward reach in patients with motor-complete injuries at level T10-T12 (23 cm) was found compared to patients with higher injuries at level C5-T4, who reached 14-16 cm.[38] The SCI patient who participated here suffered a motor-complete injury at the level of T8, having less residual motor function to reach compared to other patients with higher lesions or incomplete injuries.

Surprisingly, no correlation could be found between the functional arm reaches during the mFRT and the maximum CoP displacement during the maximum leaning task. Theoretically, both experiments evaluate a similar movement of the trunk. However, the conditions under which they were performed differed highly. During the maximum leaning task, the aim was to isolate the trunk, by removing foot support and by asking participants to prevent movement of their legs and arms. In contrast, during the mFRT the subjects could use foot support, were given no movement restrictions and used their arms to reach, which better resembles daily life conditions. Therefore, the assessment of the isolated trunk, as aimed in the maximum leaning task, might reveal different aspects of dynamic postural stability as the quantification of functional reach.

4.4 Muscle activation patterns during static leaning postures and a dynamic circular trunk movement

When moving the trunk's center of mass (CoM) in a particular direction, hip and trunk muscles must generate torque in the opposite direction to maintain stability.[61] For example, a forward shifted CoM generates a flexion torque around the hip joint and spine, which needs to be counteracted by an extension torque generated by the hip and trunk extensors to prevent the body from falling. This muscle behavior is clearly seen in the muscle activation patterns during multi-directional leaning postures and during the dynamic circular trunk movement. For both conditions, muscles were most active in the direction opposite to their function (e.g. hip extensor is most active when the hip is in flexion), as defined as antagonist activation, and muscles were more active in contralateral compared to ipsilateral directions. These activation patterns of specifically the m. Erector Spinae and the two abdominal muscles (m. Rectus Abdominis and m. Obliquus Externus) are consistent with the activation patterns found when applying multi-directional perturbations[57,62] or load to the trunk.[63] All together, antagonist and contralateral muscle activation seems to be required not only to withstand perturbations or load as seen in previous studies, but also to hold leaning postures or perform a dynamic circular trunk movement as assessed here.

Conflicting the activation patterns acquired here, the other studies clearly showed a difference in activation between the two abdominal muscles, where the m. Obliquus Externus was more active over the lateral directions compared to the m. Rectus Abdominis.[62,57,63] This difference in behavior is to be expected, since the m. Rectus Abdominis spans the trunk vertically, while fibers of the m. Obliquus Externus cross the trunk diagonally and transversely, contributing more to the lateral flexion torque of the trunk.[64] However, in our study, the two abdominal muscles behaved very similar and, in general, the activation patterns of all muscles were more distributed over the different directions. Both may be explained by the interference of cross-registration. This signal distortion, where the signal of the muscle of interest is contaminated with activity of other muscles nearby, could be caused by our monopolar EMG configuration. For each muscle of interest, one electrode was placed on the muscle and the other on a distant bony landmark. This electrode orientation causes a recording over a large area, potentially including other active muscles. The other studies, comparatively, employed bipolar electrode configuration[57,62] or intra-muscular electrodes,[63] both recording activity over a smaller area.[65] Therefore, these other methods are less sensitive for cross-registration and might have facilitated the previous studies to derive clearer distinctions between activation patterns of different muscles.

4.5 Muscle synchronization during a dynamic circular trunk movement

Intermuscular EMG-EMG coherence analysis of the EMG signals during the circular trunk movement revealed high coherence over a broad frequency band (0-100 Hz) for some neighboring muscle pairs, while coherence was absent for distant muscle pairs. The assessment of inter-muscular coherence has previously been used to reveal muscle synergies, which are combinations of muscles sharing a supraspinal neural drive in the specific frequency band where coherence is high.[66] To our knowledge, no other research reported on the intermuscular coherence between the different trunk and hip muscle pairs which we evaluated. However, muscle synergies in the legs during standing have previously been revealed, indicated by high intermuscular coherence in different frequency bands up to 50 Hz.[66] Furthermore, synchronization between the trunk and legs has been reported, as high coherences between 0-8 Hz were found in different trunk and leg muscle combinations.[67,68] Lastly, Kenville et al. were the only to evaluate a muscle synergy within the trunk, as they recorded high intermuscular coherence in 0-40 Hz between the left and right m. Erector Spinae.[69] However, to date, no studies have reported high intermuscular coherence between 60-100 Hz for muscle pairs, as we observed here. As similar to the inconsistencies in activation patterns between our and other studies, these differences in results could also be explained by the monopolar EMG configuration we used, being known to increase intermuscular coherence as it enhances the amount of cross-registration.[70,71] This might suggest that the intermuscular EMG-EMG coherence found here, especially at higher frequencies, does not only reflect relevant muscle synchronization during trunk movements, but could also reveal cross-registration between the muscle combinations.

4.6 Future use of the measurement protocol to evaluate DRG stimulation effects on postural stability

The exploration of the different aspects of healthy postural stability serves as a reference for the future long-term DRG stimulation study, where stimulation effects on postural stability in SCI patients will be evaluated. Research on spinal cord stimulation techniques, including transcutaneous spinal cord stimulation (tSCS)[72,73] and epidural spinal cord stimulation (eSCS),[74,75,76,77] as well as the pilot study on DRG stimulation,[30,30] has mainly focused on successfully regaining motor control in the legs. However, several patients included in the pilot study on DRG stimulation also reported a feeling of improved seated balance as side-effect during a 5-day stimulation period.[30] The SCI patient included in this study showed enhanced sway during upright sitting and diminished multi-directional reach and leaning distances compared to healthy individuals. Therefore, a potential stimulation-induced improvement in postural stability is expected to be quantified by smaller CoP sway during upright sitting and larger maximum reach and lean distances.

Furthermore, potential stimulation-induced changes in muscle contribution can be evaluated by assessing activation patterns and intermuscular coherence, as proposed here. DRG stimulation has the unique benefit of directly targeting DRG's of specific spinal levels. Accordingly, activation patterns of the muscles innervated by the targeted spinal levels would be expected to change during stimulation. Moreover, high intermuscular coherence between muscles in healthy individuals is often associated with a common supraspinal drive, however in SCI patients this supraspinal drive is interrupted. Therefore, an increase in intermuscular coherence after stimulation could reveal how DRG stimulation might facilitate the spinal cord to recover in transmitting supraspinal commands or how stimulation might enhance muscle synchronization within the local spinal circuitry. All together, changes in muscle activation and synchronization, with healthy muscle behavior as reference, could bring to light to what extent DRG stimulation is able to regain trunk motor control.

4.7 Recommendations for improvement of the experimental protocol

As mentioned before, the EMG signals recorded during experiments have likely been contaminated by cross-registration, due to a monopolar electrode configuration and shared reference electrodes. A bipolar electrode configuration as recommended by SENIAM,[37] could reduce cross-registration. Therefore, we performed additional measurements to compare EMG signals recorded with a monopolar and bipolar configuration. We recorded specifically the m. Rectus Abdominis and m. Obliquus Externus during 60 seconds of backward leaning, and did one measurement where we recorded all muscles during the sweep task. In line with results of Mohr et al.,[71] the bipolar configuration reduced the intermuscular coherence for all muscle pairs (see figures 15 and 17 in appendix A). Notably, a difference in coherence was seen between the sweep task and the 60 seconds of backward leaning. During the sweep task, the bipolar recordings resulted in intermuscular coherence mostly below the confidence limit. Nonetheless, the intermuscular coherence during the 60 seconds of backward leaning, clearly exceeded the confidence limit between 0-40 Hz and between 60-100 Hz. The coherence between 0-40 Hz is consistent with previous research, while a high intermuscular coherence between 60-100 Hz has never been reported yet and might still be caused by cross-registration. All-together, the bipolar EMG technique might have silenced some, however not all, cross-registration. Accordingly, a further exploration of the use of bipolar in stead of monopolar electrode configuration is recommended for future research.

Variability in anthropomorphic characteristics and experiment execution migh explain some inter-subject variability in the included population. The characteristics we collected, including total height and weight, mostly showed negligible correlation with the stability outcome measures. More specific anthropomorphic characteristics, including hip width, thigh length and trunk length, however, might have an influence on the outcome measures. Furthermore, participants differently interpreted some experiment instructions. For example, at the moment of maximum leaning, dips in vertical force (F_z) were seen in the CoP data of some participants, affecting the CoP recordings. This indicated that they used the metal frame below the seating surface partly for foot support, while we asked them to prevent touching it. Therefore future experiments could be improved by taking more anthropomorphic characteristics into account and by considering more detailed instructions, with less room for individual interpretation.

Besides experimental design, signal analysis approaches could also be of influence on our results, including choices concerning filtering and rectification prior to coherence analysis. Firstly, electrocardiogram (ECG) artifacts severely dominated the trunk EMG signals. A high-pass filter of 30 Hz silenced many of these artifacts, however, it might also have silenced some of the relevant muscle activity. Other methods to remove ECG arifacts have been proposed based on the morphology of the ECG waveform, e.g. independent component analysis, which might be better suited for trunk EMG recordings.[78,79] Furthermore, there remains debate on whether to rectify signals prior to coherence analysis or not. Since rectification is a non-linear signal processing step, some concerns exist that it might disturb the spectral content of the EMG signals in a way which can not be predicted.[80] However, research

showed that coherence analysis in rectified signals outperformed coherence analysis in unrectified signals when detecting common oscillations.[81,82] The rationale behind this finding is that common neural drive is often reflected in low frequency amplitude fluctuations, which are emphasized by rectification.[82] However, comparing coherence results with and without prior rectification, as well as the consideration of advanced filtering techniques, could be considered for future experimental design.

5 Conclusion

This study investigated postural stability in healthy individuals using a novel experimental protocol, involving the quantification of CoP excursion and muscle activity during seated stability tasks. This particular experimental protocol will also be used to quantify the effects of DRG stimulation on postural stability in SCI patients during the upcoming long-term DRG stimulation study. These potential stimulation-induced changes can in future research not only be tracked over time, but results can now also be related to postural stability in an healthy population by using the results of this study as reference.

6 Acknowledgements

This project was the definition of multidisciplinary collaboration, which I highly enjoyed. PhD-candidate Sadaf Soloukey and neurosurgeon Sanjay Harhanghi, in collaboration with colleagues from the Center of Pain Medicine, were those who started the work on the employment of DRG-stimulation to evoke motor responses in SCI patients. Their work has already led to multiple published papers providing first evidence that DRG stimulation can evoke motor responses in paralyzed legs. That promising work also led to the hypothesis that DRG stimulation could be used to regain postural stability in SCI patients. That is where I stepped in a year ago, when I started an internship at the department of Neurosurgery under the supervision of Sadaf Soloukey, Sanjay Harhangi and Cecile de Vos to help prepare postural stability experiments for the long-term DRG stimulation study. I also met Tiago Beck, a fellow student on the project, who soon became my team mate and friend and with who I shared joys and sorrows over the last year. We worked closely together on almost all aspects of the project. Therefore, we could help each other out a lot, but it also just made the project a lot more fun.

I was so intrigued by the project, that I asked Cecile, Sanjay and Sadaf to extend my work done in the internship to my graduation project, which they allowed. I would really like to thank them all for their enthusiasm and critical stance throughout the whole project. Sanjay, and his colleagues, learned me also a lot about the field of neurosurgery. I got the opportunity to talk to patients, learn what they go through, link that to physiology and pathology of the CNS, and experience what treatments could be offered to relieve symptoms and improve quality of life. Cecile, as my technical supervisor, always pushed me to improve my work, dive into subjects a little deeper and make well-informed decisions. I really liked our coffee meetings or walks through Rotterdam Noord where we thoroughly discussed project planning, experimental design and analysis approaches. Furthermore, we were allowed to use the force plate from Patrick Forbes and as the time passed, Patrick became more invested in the project. With his expertise in research on human balancing, he was able to shed new light on our experimental designs and signal analysis approaches. This resulted in having multiple meetings a week for the last few months, which I really enjoyed since I learned a lot about biomechanics, EMG measurement techniques and correlation analysis.

I would also like to thank the department of Clinical Neurophyisiology for allowing us to use their equipment and examination rooms for the measurements, but also for their assistance in making the experiments possible. We really asked a lot of flexibility from them, since we encountered many obstacles during testing which required us to revise the measurement set-up and repeat test measurements multiple times. However, they were always willing to help us fix the issues to bring the project further. Specifically, neurologist Judith Drenthen learned us a lot about the theory behind EMG measurements and guided us in preparing the EMG recordings. Furthermore, Venny Pires was always available to help with practical matters, like reserving examination rooms, use of equipment and use of the EMG protocol. Lastly, Marc de Geer was invaluable in the design of the measurement set-up to simultaneously record EMG and force plate data. His door was always open to help us with set-up design, connector problems, recording issues, and so forth, while learning us a lot about electrical circuits.

Last but not least, I want to thank everyone who was willing to come to the Erasmus MC, usually on weekend days, to participate in my experiments. I highly appreciate the enthusiasm and interest they all showed.

References

[1] J Hb Nijendijk, M Wm Post, and F Wa Van Asbeck. “Epidemiology of traumatic spinal cord injuries in The Netherlands in 2010”. In: *Spinal cord* 52.4 (2014), pp. 258–263.

[2] Kim D Anderson. “Targeting recovery: priorities of the spinal cord-injured population”. In: *Journal of neurotrauma* 21.10 (2004), pp. 1371–1383.

[3] Vernon W Lin et al. *Spinal cord medicine: principles and practice*. Demos medical publishing, 2010.

[4] Nicholas R Heebner et al. “Reliability and validity of an accelerometry based measure of static and dynamic postural stability in healthy and active individuals”. In: *Gait & posture* 41.2 (2015), pp. 535–539.

[5] HAM Seelen et al. “Impaired balance control in paraplegic subjects”. In: *Journal of Electromyography and Kinesiology* 7.2 (1997), pp. 149–160.

[6] YJM Potten et al. “Postural muscle responses in the spinal cord injured persons during forward reaching”. In: *Ergonomics* 42.9 (1999), pp. 1200–1215.

[7] Douglas A Hobson and ROBERT E Tooms. “Seated lumbar/pelvic alignment. A comparison between spinal cord-injured and noninjured groups.” In: *Spine* 17.3 (1992), pp. 293–298.

[8] Jean L Minkel. “Seating and mobility considerations for people with spinal cord injury”. In: *Physical therapy* 80.7 (2000), pp. 701–709.

[9] R Vialle, C Thévenin-Lemoine, and P Mary. “Neuromuscular scoliosis”. In: *Orthopaedics & Traumatology: Surgery & Research* 99.1 (2013), S124–S139.

[10] Robert J Peterka. “Sensory integration for human balance control”. In: *Handbook of clinical neurology* 159 (2018), pp. 27–42.

[11] José A Vega and Juan Cobo. “Structural and Biological Basis for Proprioception”. In: *Proprioception*. IntechOpen, 2021.

[12] David F Collins et al. “Cutaneous receptors contribute to kinesthesia at the index finger, elbow, and knee”. In: *Journal of neurophysiology* 94.3 (2005), pp. 1699–1706.

[13] David Burke and Göran Eklund. “Muscle spindle activity in man during standing”. In: *Acta Physiologica Scandinavica* 100.2 (1977), pp. 187–199.

[14] Tatiana G Deliagina et al. “Neural bases of postural control”. In: *Physiology* 21.3 (2006), pp. 216–225.

[15] Robert M Brownstone, Tuan V Bui, and Nicolas Stifani. “Spinal circuits for motor learning”. In: *Current opinion in neurobiology* 33 (2015), pp. 166–173.

[16] R Cornet et al. “Tablet Technology for Rehabilitation after Spinal Cord Injury: a Proof-of-Concept”. In: (2015).

[17] Madhusree Sengupta et al. “Role of virtual reality in balance training in patients with spinal cord injury: a prospective comparative pre-post study”. In: *Asian spine journal* 14.1 (2020), p. 51.

[18] Martha M Sliwinski et al. “Community exercise programing and its potential influence on quality of life and functional reach for individuals with spinal cord injury”. In: *The Journal of Spinal Cord Medicine* 43.3 (2020), pp. 358–363.

[19] Jessica M Leathem et al. “Community exercise for individuals with spinal cord injury with inspiratory muscle training: A pilot study”. In: *The Journal of Spinal Cord Medicine* (2019), pp. 1–9.

[20] Laura A Rice et al. “A brief fall prevention intervention for manual wheelchair users with spinal cord injuries: A pilot study”. In: *The journal of spinal cord medicine* 43.5 (2020), pp. 607–615.

[21] Tanja Herzog et al. “Effect of indoor wheelchair curling training on trunk control of person with chronic spinal cord injury: a randomised controlled trial”. In: *Spinal cord series and cases* 4.1 (2018), pp. 1–6.

[22] Anna Bjerkefors, MG Carpenter, and Alf Thorstensson. “Dynamic trunk stability is improved in paraplegics following kayak ergometer training”. In: *Scandinavian journal of medicine & science in sports* 17.6 (2007), pp. 672–679.

[23] Amanda E Chisholm et al. “Overground vs. treadmill-based robotic gait training to improve seated balance in people with motor-complete spinal cord injury: a case report”. In: *Journal of neuroengineering and rehabilitation* 14.1 (2017), p. 27.

[24] Anu Piira et al. “Robot-assisted locomotor training did not improve walking function in patients with chronic incomplete spinal cord injury: a randomized clinical trial”. In: *Journal of rehabilitation medicine* 51.5 (2019), pp. 67–71.

[25] Mrinal Rath et al. “Trunk stability enabled by noninvasive spinal electrical stimulation after spinal cord injury”. In: *Journal of neurotrauma* 35.21 (2018), pp. 2540–2553.

[26] Julie O Murphy et al. “Feasibility of closed-loop controller for righting seated posture after spinal cord injury”. In: *J Rehabil Res Dev* 51.5 (2014), pp. 747–760.

[27] Musa L Audu et al. “A neuroprosthesis for control of seated balance after spinal cord injury”. In: *Journal of neuroengineering and rehabilitation* 12.1 (2015), p. 8.

[28] Ronald J Triolo et al. “Implanted electrical stimulation of the trunk for seated postural stability and function after cervical spinal cord injury: a single case study”. In: *Archives of physical medicine and rehabilitation* 90.2 (2009), pp. 340–347.

[29] Sahana N Kukke and Ronald J Triolo. “The effects of trunk stimulation on bimanual seated workspace”. In: *IEEE Transactions on neural systems and rehabilitation engineering* 12.2 (2004), pp. 177–185.

[30] Sadaf Soloukey et al. “The Dorsal Root Ganglion as a Novel Neuromodulatory Target to Evoke Strong and Reproducible Motor Responses in Chronic Motor Complete Spinal Cord Injury: A Case Series of Five Patients”. In: *Neuromodulation: Technology at the Neural Interface* (2020).

[31] Keith L Moore, Anne MR Agur, Arthur F Dalley, et al. “Essential clinical anatomy”. In: (2015).

[32] Mark A Mahan et al. “Anatomy of psoas muscle innervation: cadaveric study”. In: *Clinical Anatomy* 30.4 (2017), pp. 479–486.

[33] Josephine Dumas. *Literature review: The quantification of postural stability in spinal cord injury patients undergoing stability-improving interventions*. 2020.

[34] Martin L Tanaka, Shane D Ross, and Maury A Nussbaum. “Mathematical modeling and simulation of seated stability”. In: *Journal of biomechanics* 43.5 (2010), pp. 906–912.

[35] AL Hof, MGJ Gazendam, and WE Sinke. “The condition for dynamic stability”. In: *Journal of biomechanics* 38.1 (2005), pp. 1–8.

[36] Walter F Boron and Emile L Boulpaep. *Medical physiology E-book*. Elsevier Health Sciences, 2016.

[37] D Stegeman and H Hermens. “Standards for surface electromyography: The European project Surface EMG for non-invasive assessment of muscles (SENIAM)”. In: *Enschede: Roessingh Research and Development* (2007), pp. 108–12.

[38] Suzanne M Lynch, Patricia Leahy, and Susan P Barker. “Reliability of measurements obtained with a modified functional reach test in subjects with spinal cord injury”. In: *Physical therapy* 78.2 (1998), pp. 128–133.

[39] Sadaf Soloukey et al. “How to Identify Responders and Nonresponders to Dorsal Root Ganglion-Stimulation Aimed at Eliciting Motor Responses in Chronic Spinal Cord Injury: Post Hoc Clinical and Neurophysiological Tests in a Case Series of Five Patients”. In: *Neuromodulation: Technology at the Neural Interface* (2021).

[40] Sunghoon Shin and Jacob J Sosnoff. “Spinal cord injury and seated postural control: a test of the rambling and trembling hypothesis”. In: *Motor control* 21.4 (2017), pp. 443–456.

[41] Josephine Dumas. *Internship report: Dorsal root ganglion stimulation in motor-complete spinal cord injury patients: development of a measurement system and data-analysis protocol to quantify its effect on postural stability*. 2020.

[42] Aldo O Perotto. *Anatomical guide for the electromyographer: the limbs and trunk*. Charles C Thomas Publisher, 2011.

[43] Matija Milosevic et al. "Trunk control impairment is responsible for postural instability during quiet sitting in individuals with cervical spinal cord injury". In: *Clinical Biomechanics* 30.5 (2015), pp. 507–512.

[44] Albert H Vette et al. "Posturographic measures in healthy young adults during quiet sitting in comparison with quiet standing". In: *Medical engineering & physics* 32.1 (2010), pp. 32–38.

[45] Thomas E Prieto et al. "Measures of postural steadiness: differences between healthy young and elderly adults". In: *IEEE Transactions on biomedical engineering* 43.9 (1996), pp. 956–966.

[46] Murielle Grangeon et al. "Effects of upper limb positions and weight support roles on quasi-static seated postural stability in individuals with spinal cord injury". In: *Gait & posture* 36.3 (2012), pp. 572–579.

[47] Sunghoon Shin and Jacob J Sosnoff. "Spinal cord injury and time to instability in seated posture". In: *Archives of physical medicine and rehabilitation* 94.8 (2013), pp. 1615–1620.

[48] Mavuto M Mukaka. "A guide to appropriate use of correlation coefficient in medical research". In: *Malawi medical journal* 24.3 (2012), pp. 69–71.

[49] Matija Milosevic et al. "Muscle synergies reveal impaired trunk muscle coordination strategies in individuals with thoracic spinal cord injury". In: *Journal of Electromyography and Kinesiology* 36 (2017), pp. 40–48.

[50] Dario Farina, Francesco Negro, and Ning Jiang. "Identification of common synaptic inputs to motor neurons from the rectified electromyogram". In: *The Journal of physiology* 591.10 (2013), pp. 2403–2418.

[51] David M. Halliday. *NeuroSpec 2.11. Guide.* Copyright©2016.

[52] David Slepian. "Prolate spheroidal wave functions, Fourier analysis, and uncertainty—V: The discrete case". In: *Bell System Technical Journal* 57.5 (1978), pp. 1371–1430.

[53] Donald B Percival, Andrew T Walden, et al. *Spectral analysis for physical applications*. cambridge university press, 1993.

[54] Jeffrey Park, Craig R Lindberg, and Frank L Vernon III. "Multitaper spectral analysis of high-frequency seismograms". In: *Journal of Geophysical Research: Solid Earth* 92.B12 (1987), pp. 12675–12684.

[55] DM Halliday et al. "A framework for the analysis of mixed time series/point process data-theory and application to the study of physiological tremor, single motor unit discharges and electromyograms". In: *Progress in biophysics and molecular biology* 64.2 (1995), p. 237.

[56] Heather M Kerr and Janice J Eng. "Multidirectional measures of seated postural stability". In: *Clinical Biomechanics* 17.7 (2002), pp. 555–557.

[57] Richard Preuss and Joyce Fung. "Musculature and biomechanics of the trunk in the maintenance of upright posture". In: *Journal of Electromyography and Kinesiology* 18.5 (2008), pp. 815–828.

[58] HAM Seelen et al. "Postural motor programming in paraplegic patients during rehabilitation". In: *Ergonomics* 41.3 (1998), pp. 302–316.

[59] Yvonne J Janssen-Potten et al. "The effect of seat tilting on pelvic position, balance control, and compensatory postural muscle use in paraplegic subjects". In: *Archives of physical medicine and rehabilitation* 82.10 (2001), pp. 1393–1402.

[60] Priyanka Singh, Nangteidor Hujon, et al. "Normative data of Modified Functional Reach Test in younger and middle-aged North Eastern Indian population". In: *Archives of Medicine and Health Sciences* 1.2 (2013), p. 109.

[61] Ronald Huston. *Principles of biomechanics*. CRC press, 2008.

[62] Kei Masani et al. “Postural reactions of the trunk muscles to multi-directional perturbations in sitting”. In: *Clinical Biomechanics* 24.2 (2009), pp. 176–182.

[63] Martin Eriksson Crommert et al. “Directional preference of activation of abdominal and paraspinal muscles during position-control tasks in sitting”. In: *Journal of Electromyography and Kinesiology* 35 (2017), pp. 9–16.

[64] Ian AF Stokes and Mack Gardner-Morse. “Quantitative anatomy of the lumbar musculature”. In: *Journal of biomechanics* 32.3 (1999), pp. 311–316.

[65] K Roeleveld et al. “The motor unit potential distribution over the skin surface and its use in estimating the motor unit location”. In: *Acta physiologica scandinavica* 161.4 (1997), pp. 465–472.

[66] Tjeerd W Boonstra et al. “Muscle networks: Connectivity analysis of EMG activity during postural control”. In: *Scientific reports* 5.1 (2015), pp. 1–14.

[67] Adriana M Degani, Charles T Leonard, and Alessander Danna-dos-Santos. “The use of intermuscular coherence analysis as a novel approach to detect age-related changes on postural muscle synergy”. In: *Neuroscience letters* 656 (2017), pp. 108–113.

[68] Alessander Danna-Dos-Santos et al. “The influence of visual information on multi-muscle control during quiet stance: a spectral analysis approach”. In: *Experimental brain research* 233.2 (2015), pp. 657–669.

[69] Rouven Kenville et al. “Intermuscular coherence between homologous muscles during dynamic and static movement periods of bipedal squatting”. In: *Journal of Neurophysiology* 124.4 (2020), pp. 1045–1055.

[70] Bert-Ulrich Kleine et al. “Surface EMG mapping of the human trapezius muscle: the topography of monopolar and bipolar surface EMG amplitude and spectrum parameters at varied forces and in fatigue”. In: *Clinical neurophysiology* 111.4 (2000), pp. 686–693.

[71] Maurice Mohr et al. “Intermuscular coherence between surface EMG signals is higher for monopolar compared to bipolar electrode configurations”. In: *Frontiers in physiology* 9 (2018), p. 566.

[72] Yury P Gerasimenko et al. “Noninvasive reactivation of motor descending control after paralysis”. In: *Journal of neurotrauma* 32.24 (2015), pp. 1968–1980.

[73] Yury Gerasimenko et al. “Transcutaneous electrical spinal-cord stimulation in humans”. In: *Annals of physical and rehabilitation medicine* 58.4 (2015), pp. 225–231.

[74] Susan Harkema et al. “Effect of epidural stimulation of the lumbosacral spinal cord on voluntary movement, standing, and assisted stepping after motor complete paraplegia: a case study”. In: *The Lancet* 377.9781 (2011), pp. 1938–1947.

[75] Claudia A Angeli et al. “Altering spinal cord excitability enables voluntary movements after chronic complete paralysis in humans”. In: *Brain* 137.5 (2014), pp. 1394–1409.

[76] Enrico Rejc et al. “Effects of stand and step training with epidural stimulation on motor function for standing in chronic complete paraplegics”. In: *Journal of neurotrauma* 34.9 (2017), pp. 1787–1802.

[77] Megan L Gill et al. “Neuromodulation of lumbosacral spinal networks enables independent stepping after complete paraplegia”. In: *Nature medicine* 24.11 (2018), pp. 1677–1682.

[78] Joseph NF Mak, Yong Hu, and Keith DK Luk. “An automated ECG-artifact removal method for trunk muscle surface EMG recordings”. In: *Medical engineering & physics* 32.8 (2010), pp. 840–848.

[79] AL Hof. “A simple method to remove ECG artifacts from trunk muscle EMG signals.” In: *Journal of electromyography and kinesiology: official journal of the International Society of Electrophysiological Kinesiology* 19.6 (2009), e554–5.

[80] Verity M McClelland, Zoran Cvetkovic, and Kerry R Mills. “Inconsistent effects of EMG rectification on coherence analysis”. In: *The Journal of physiology* 592.Pt 1 (2014), p. 249.

[81] Tjeerd W Boonstra and Michael Breakspear. “Neural mechanisms of intermuscular coherence: implications for the rectification of surface electromyography”. In: *Journal of Neurophysiology* 107.3 (2012), pp. 796–807.

[82] Christopher J Dakin et al. “Rectification is required to extract oscillatory envelope modulation from surface electromyographic signals”. In: *Journal of neurophysiology* 112.7 (2014), pp. 1685–1691.

Appendices

A Electromyography recordings

Placement of EMG electrodes

To record EMG signals for each muscle, one active electrode was placed on the muscle belly and one reference electrode on non-electrical active structure nearby. In table 2, the locations of all electrodes are described, which were chosen based on on the Anatomical guide for the electromyographer.[42] The m. Rectus Abdominis and m. Obliquus Externus, as well as the m. Gluteus Maximus and m. Illiopsoas, had a shared reference electrode.

Muscle	Active electrode	Reference electrode
m. Erector Spinae	Two finger-breadth's lateral to processus spinosus of vertebra L3/L4 (at height of top iliac crest)	Processus spinosus of vertebra cranial of vertebra L3/L4
m. Rectus Abdominis	Two finger-breadth's lateral of abdominal midline at height of anterior superior iliac spine (ASIS)	ASIS
m. Obliquus Externus	Two finger-breadth's cranial of the midpoint of the line intersecting from the top iliac crest to the ASIS	ASIS
m. Gluteus Maximus	Midway between top iliac crest and sacral vertebrae	Greater trochanter
m. Illiopsoas	Two finger-breadth's lateral of the femoral artery	Greater trochanter

Table 2: Surface electromyography (EMG) electrode locations. Active electrode is placed on the muscle belly and the reference electrode at a near bony landmark.

Comparison monopolar and bipolar EMG configurations

In this research, monopolar recordings were used to derive EMG signals for each muscle. The signals were collected with channels originally used for electroencelography (EEG) recordings, meaning that signals of each electrode were differentially amplified in the hardware with respect to the Fz electrode, placed at the top of the head, to retrieve the monopolar recordings (see figure 14a). The two monopolar recordings were thereafter subtracted to eachother in the software, to get the resultant EMG signal, being the difference in electrical activation between the active electrode and reference electrode. However, this technique might have caused some cross-registration, as indicated by the high intermuscular coherence and distributed activation patterns found here, inconsistent with other research. Therefore, we did additional measurements in a healthy subject to compare the monopolar electrode configuration with bipolar electrode configurations, often used in other EMG research.

In figure 14 the original electrode configuration is shown (a) and two other configurations with bipolar electrode placement. The difference between monopolar and bipolar electrode placement is that monopolar placement involves one electrode on the muscle belly and one reference at a distant location, whereas for bipolar electrode placement both electrodes are on the muscle belly within two cm of each other (b and c). Furthermore, the

difference in activity between the electrode signals can be assessed by using the EEG channels to retrieve monopolar recordings (b), similar to the original technique, or by using bipolar channels to retrieve bipolar recordings (c), so that the two signals are differentially amplified with respect to each other in stead of separately with respect to Fz.

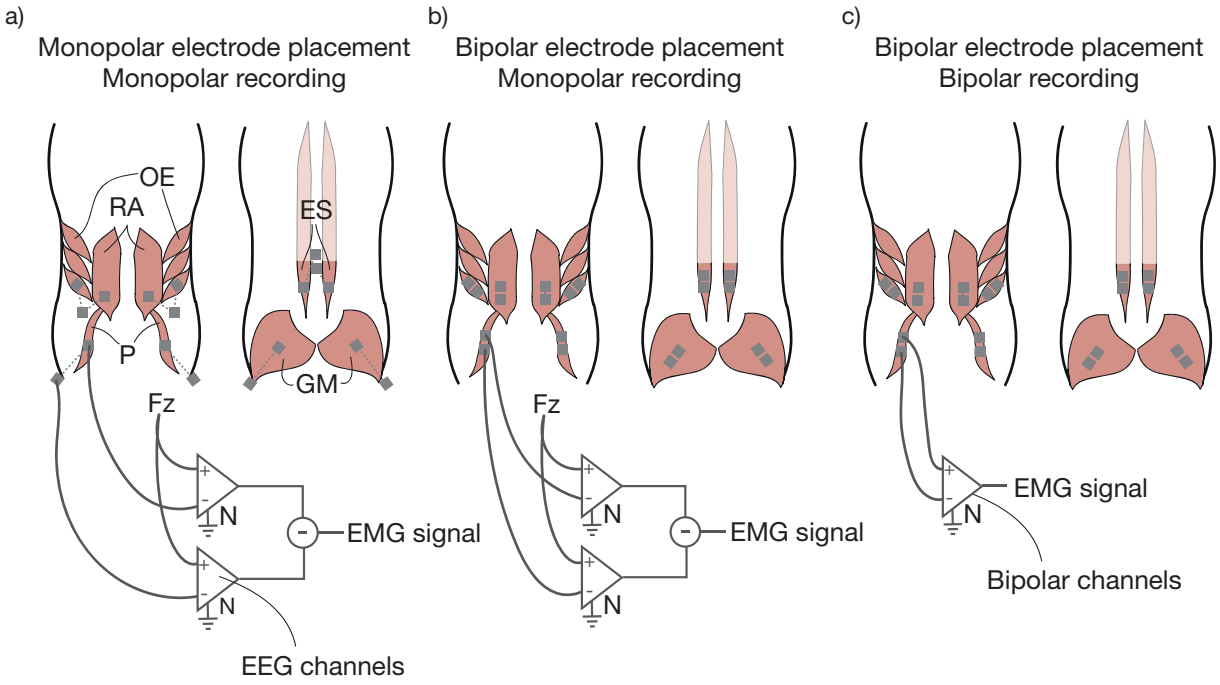

Figure 14: Three different techniques to record electromyography (EMG) signals. a) For each muscle, one active electrode is placed on the muscle belly, and one as reference on a bony landmark (see table 2 for detailed locations). The EMG signal is the result of the difference between the two monopolar recordings, which are derived by differential amplification in the hardware of the EEG channels with respect to the Fz electrode. b) For each muscle, two electrodes are placed on the muscle, within two cm of each other. EMG signal is similar derived as in a). c) For each muscle, electrodes are placed similar as in b) but the EMG signal is derived by differential amplification of both electrode signals to derive a direct bipolar recording.

Comparison of different EMG configurations in the abdominal muscles during 60s backward leaning

Intermuscular coherence was specifically high between the m. Rectus Abdominis and m. Obliquus Externus. Since they shared a shared reference electrode, the chance of cross-registration was high for these muscles. Therefore, we compared the spectral content of the EMG signals between the monopolar configuration and two bipolar configurations during trials of 60 seconds backward leaning. Figure 15 shows the results. For both muscles, all three power spectra showed a similar shape, where power decreases with higher frequency, but increases after 60 Hz to reach a peak around 100 Hz. The power is higher over all frequencies for the monopolar configuration compared to the bipolar configuration. Furthermore, the monopolar configuration resulted in higher coherence between the two abdominal muscles. Where the monopolar recordings resulted in coherence exceeding the confidence limit up to 400 Hz, the coherence of the bipolar recordings dropped below the limit after 100 Hz.

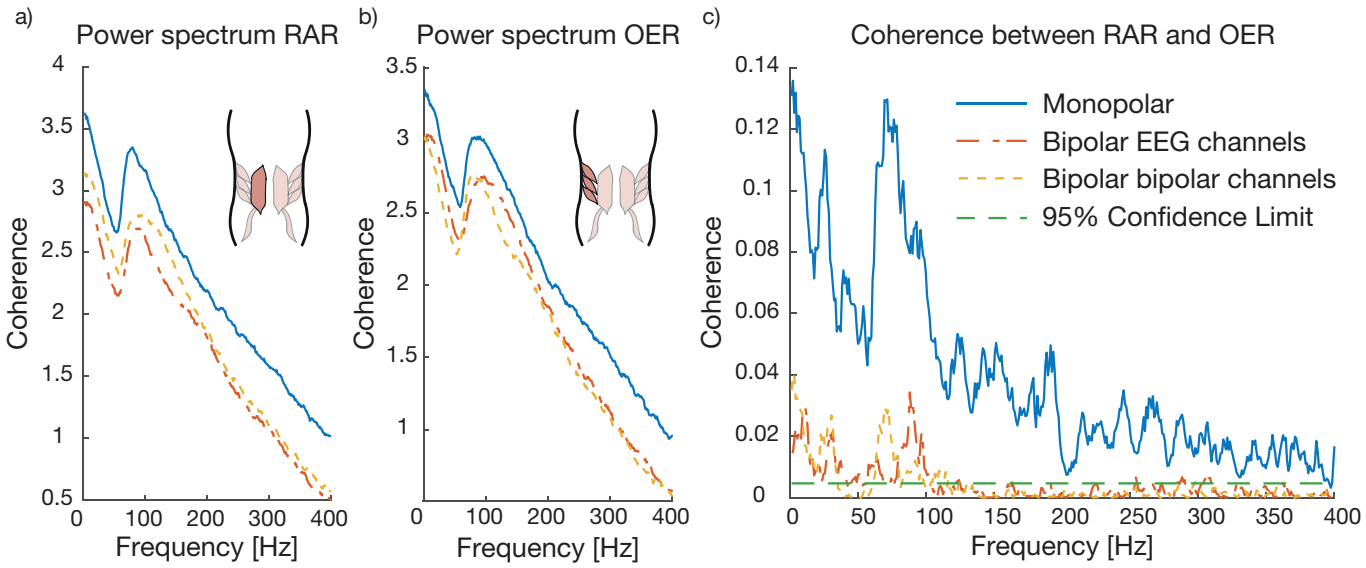

Figure 15: Spectral content of EMG signals of the m. Rectus Abdominis (RAR) and m. Obliquus Externus (OER), recorded using monopolar electrode configuration, bipolar configuration with EEG channels and bipolar configuration with bipolar channels (see figure 14). a) and b) Power spectra of the two muscles. c) Intermuscular coherence between the two muscles. Significant coherence is indicated by the dotted green line, indicating the 95% confidence limit.

Muscle activation patterns and intermuscular coherence retrieved from EMG recordings using bipolar configuration

EMG of all muscles was recorded during the sweep task using the bipolar configurations, so that results could be compared to the group averages retrieved with the monopolar configuration. Figure 16 shows the muscle activation patterns as retrieved by the two new bipolar configurations. Since only bipolar channels were available for six muscles, we chose to only record EMG with the bipolar channels for the five right muscles to test the bipolar channels, with the five left muscles being recorded with the EEG channels. Figure 16 shows the activation patterns as recorded with the biopolar EMG configurations. The patterns do not reveal clear differences when comparing to the monopolar configuration (see figure 12). However, it is difficult to compare this result from one subject with the results of a group of 20 subjects with high inter-subject variability. Moreover, figure 17 shows the intermuscular coherence between EMG signals recorded with the bipolar configurations, with the coherences being way lower than the group average and individual coherences found with the monopolar configuration (see figure 13). Furthermore, where the monopolar configuration resulted in coherence exceeding the confidence limit between 0-100 Hz, the coherence plots of bipolar configurations are characterized by some peaks exceeding the confidence limit. Notably, when looking at the coherence between the two abdominal muscles, the increase in coherence between 60-100 Hz, as seen during backward leaning (see figure 15) is absent during the circular trunk movement.

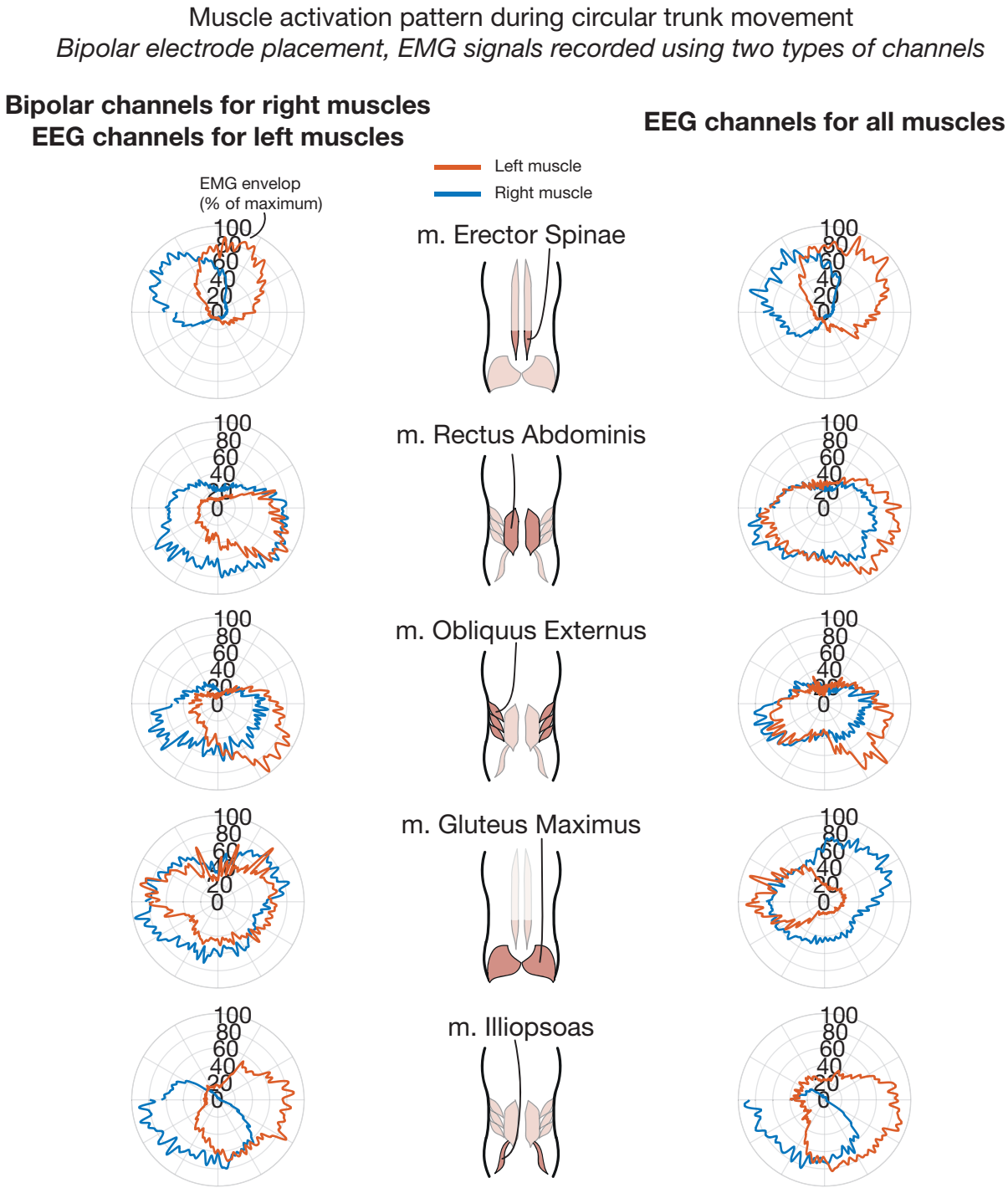

Figure 16: Muscle activation pattern of an healthy subject during a counter-clockwise circular trunk movement, derived from electromyography (EMG) recordings using bipolar electrode placement and two different types of channels for recording. Results from a measurement using bipolar channels for the right muscles and electroencelography (EEG) channels for the left muscles (left), and from a measurement using EEG channels for all muscles (right) are shown.

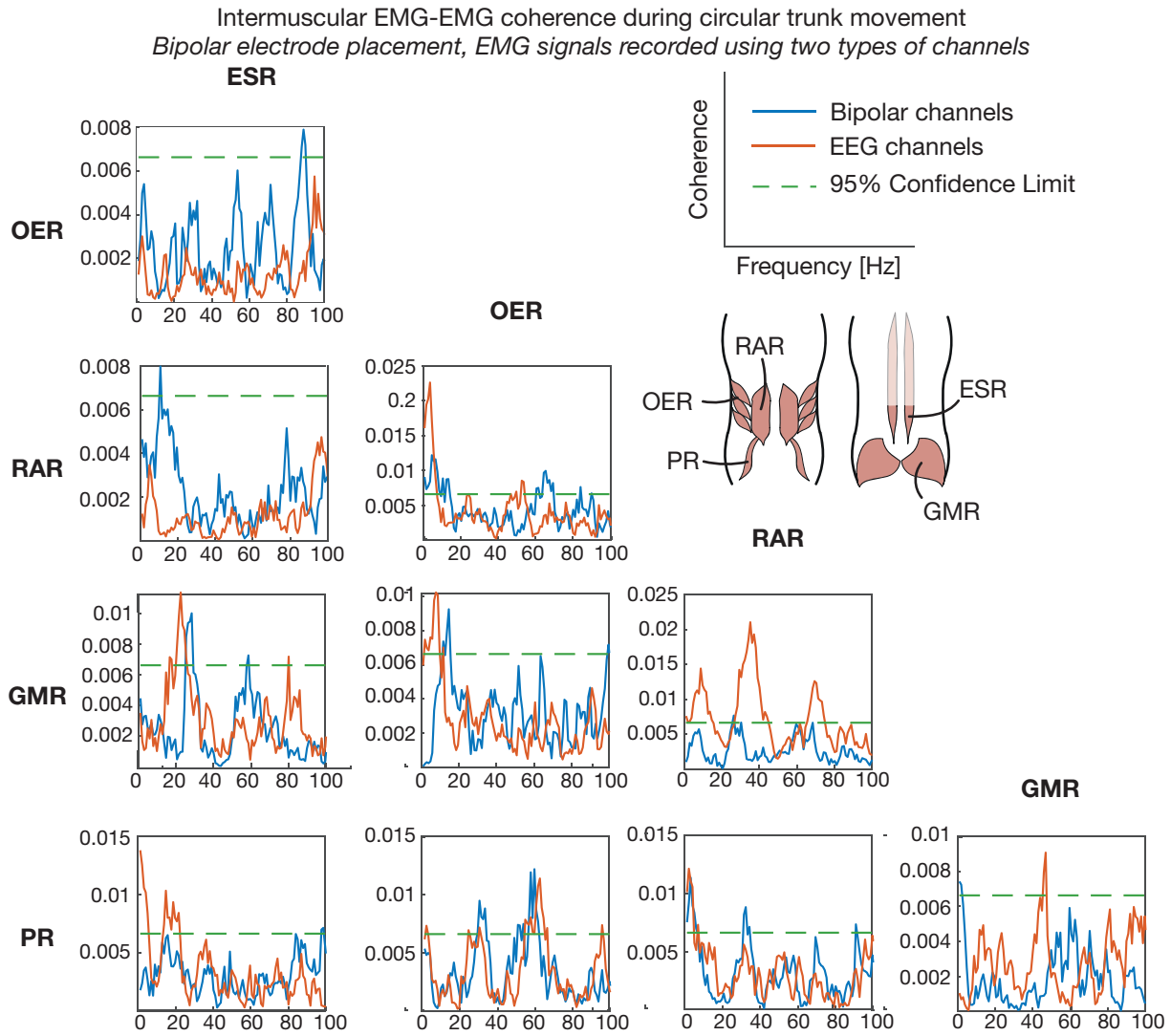

Figure 17: Intermuscular coherence of all combinations of the five right muscles during one counter-clockwise circular movement in one healthy individual, derived from electromyography (EMG) recordings using bipolar electrode placement and two different types of channels for recording (bipolar channels and electroencelography (EEG) channels). Coherence between right trunk and hip muscle pairs is shown. The limit of significant coherence is indicated by the green dotted line, representing the 95 % confidence limit. ESR = right m. Erector Spinae, OER = right m. Olbiquus Externus, RAR = right m. Rectus Abdominis, GMR = right m. Gluteus Maximusr, PR = right m. Illiopsoas

B Results - CoP sway characteristics

Table 3: Outcome measures retrieved from center of pressure (CoP) displacement data during the static upright sitting task for every participant. Displayed values per participant are the outcomes for all three 30 seconds runs (smallest to highest). RMS = root-mean-square. CI = confidence interval. SCI = spinal cord injury.

Healthy subject	**RMS CoP displacement [mm]**			**RMS CoP velocity [mm/s]**			**RMS CoP acceleration [mm/s/s]**		
1	0.8	0.9	1.0	3.2	3.6	3.9	111	118	133
2	1.1	1.3	1.3	7.3	7.4	7.6	244	295	320
3	1.0	1.3	1.3	2.9	3.0	3.3	87	90	111
4	0.9	1.2	1.2	3.4	3.5	3.8	99	109	124
5	1.1	1.4	1.6	6.2	7.3	7.5	267	282	286
6	0.9	1.0	1.2	5.7	6.2	6.7	237	263	263
7	0.8	1.1	1.1	3.9	4.5	4.6	122	158	174
8	0.8	0.9	0.9	4.6	4.6	5.1	204	219	289
9	1.1	1.1	1.2	7.1	7.2	7.2	259	269	387
10	0.9	1.0	1.1	3.6	4.4	4.8	107	160	192
11	0.7	0.9	1.0	3.1	3.2	3.6	97	114	150
12	0.8	0.8	1.7	4.8	5.0	5.3	159	206	242
13	0.9	0.9	1.3	3.4	3.5	4.3	130	138	175
14	0.7	0.7	0.8	3.0	3.0	3.5	110	117	154
15	0.6	0.6	0.8	4.5	4.6	5.0	185	220	234
17	0.7	1.3	1.4	3.7	3.8	4.2	120	122	139
18	0.9	0.9	1.2	3.4	4.6	4.9	117	156	185
19	0.6	0.7	1.1	2.4	2.5	2.8.	77	80	88
20	0.7	0.9	1.0	4.0	4.1	4.7	137	149	193
Men average (1-10) (95% CI)	**1.1 (1.0 - 1.2)**			**5.1 (4.2 - 6.0)**			**199 (154 - 244)**		
Women average (11-20) (95% CI)	**0.9 (0.8 - 1.0)**			**3.89 (3.5 - 4.3)**			**148 (128 - 168)**		
Group average (95% CI)	**1.0 (0.9 - 1.1)**			**4.5 (4.0 - 5.0)**			**175 (149 - 201)**		
SCI patient									
1	1.2	1.6	2.1	3.3	3.5	3.7	72	78	81
SCI average	**1.6**			**3.5**			**72**		

C Results - Maximum CoP displacements during leaning

Table 4: Maximum center of pressure (CoP) displacement for every participant during the maximum reach task. Displayed values are the mean of three trials for every direction. In figure 9 the eight directions are visualized.

	Maximum CoP displacement [cm]							
Healthy subject	**N**	**NE**	**E**	**SE**	**S**	**SW**	**W**	**NW**
1	14.6	17.2	13.2	16.5	18.5	14.2	10.8	17.2
2	25.6	22.3	13.3	15.9	15.5	12.6	11.3	21.0
4	12.8	15.4	10.1	12.1	11.9	12.4	11.0	15.1
5	18.7	17.0	10.9	12.6	13.0	11.8	10.5	18.0
6	19.0	17.7	13.9	15.1	15.3	14.6	12.3	15.4
7	15.2	15.8	10.2	10.9	10.6	13.2	12.1	16.9
8	16.0	16.8	12.5	15.5	18.6	16.3	11.5	16.2
9	19.5	18.9	11.5	16.1	20.0	18.5	15.0	20.8
10	18.1	18.6	12.7	15.6	19.7	16.4	12.2	19.4
11	12.1	13.7	8.5	12.2	15.2	13.9	9.1	13.9
12	13.5	15.2	10.3	12.1	12.1	13.7	13.0	15.0
13	18.3	16.4	13.7	19.4	16.8	15.5	12.2	17.2
14	10.0	8.5	7.9	9.0	10.0	9.6	8.4	10.2
15	13.2	11.3	8.1	10.4	10.0	10.9	7.9	12.3
17	12.7	13.7	12.4	15.3	19.3	15.5	9.6	12.0
18	19.1	22.2	15.6	20.9	18.8	18.5	13.6	20.0
19	15.2	14.2	12.1	14.7	15.6	15.8	13.2	15.4
20	18.1	19.4	11.9	17.7	16.0	17.5	13.9	20.5
Men average (95% CI)	**17.7 (15.9-19.5)**	**17.7 (16.8-18.7)**	**12.0 (11.2-12.8)**	**14.5 (13.3-15.6)**	**15.9 (14.0-17.8)**	**14.4 (13.3-15.6)**	**11.8 (11.2-12.5)**	**17.8 (16.6-19.0)**
Women average (95% CI)	**14.7 (13.0-16.4)**	**15.0 (13.0-16.9)**	**11.2 (9.7-12.6)**	**14.6 (12.5-16.8)**	**14.9 (13.1-16.7)**	**14.6 (13.1-16.0)**	**11.2 (9.8-12.7)**	**15.2 (13.4-17.0)**
Group average (95% CI)	**16.2 (14.8-17.6)**	**16.4 (15.2-17.5)**	**11.6 (10.8-12.4)**	**14.6 (13.4-15.7)**	**15.4 (14.1-16.7)**	**14.5 (13.6-15.4)**	**11.5 (10.8-12.2)**	**16.5 (15.3-17.6)**
SCI patient								
1	3.6	5.0	2.9	2.6	3.2	3.3	3.8	3.5

D Results - Modified Functional Reach Test

Table 5: Maximum reaching distance for every participant during the modified Functional Reach Test (mFRT). Displayed values are the mean of three trials for every direction.

Healthy subject	**Forward reach [cm]**	**Left lateral reach [cm]**	**Right lateral reach [cm]**
1	47	25	34
2	62	48	44
3	41	34	25
4	50	25	25
5	49	29	32
6	47	28	35
7	53	31	27
8	47	28	29
9	41	24	26
10	52	34	38
11	56	35	35
12	50	36	28
13	34	25	25
14	41	28	30
15	51	26	30
16	48	33	31
17	49	27	28
18	51	26	22
19	48	28	38
20	54	37	35
Group average (95% CI)	**49 (47 - 50)**	**30 (28-32)**	**31 (29-33)**
SCI patient			
1	11	17	22

E Pearson correlation coefficients

Generally, Pearson correlation coefficient define the correlation strength as follows:[48]

- 0.0 - 0.3: Negligible correlation
- 0.3 - 0.5: Low correlation
- 0.5 - 0.7: Moderate correlation
- 0.7 - 0.9: High correlation
- 0.9 - 1.0: Very high correlation

Table 6: Pearson correlation coefficients between CoP sway characteristics during quiet sitting and participant characteristics

	RMS displacement	**RMS velocity**	**acceleration**
Age	0.01	-0.43	-0.51
Height	0.24	0.27	0.21
Weight	0.46	-0.02	-0.15

Table 7: Pearson correlation coefficients between maximum CoP displacements during maximum leaning task and participant characteristics

	N	**NE**	**E**	**SE**	**S**	**SW**	**W**	**NW**
Age	0.15	0.33	0.27	0.19	0.43	0.39	0.26	0.30
Height	0.34	0.30	0.05	-0.07	0.01	-0.01	0.09	0.36
Weight	-0.11	0.14	0.38	0.31	0.52	0.45	0.17	0.09

Table 8: Pearson correlation coefficients between maximum arm reaches during mFRT and participant characteristics

	Forward	**Left**	**Right**
Age	-0.03	-0.24	-0.15
Height	0.12	-0.01	0.13
Weight	0.03	-0.15	-0.19

Table 9: Pearson correlation coefficients between maximum CoP displacements during maximum leaning task and maximum arm reaches during mFRT

	Forward	**Left**	**Right**
N	0.23		
W		0.04	
E			0.02